Published for SISSA by Springer

Received: *September 14, 2016*
Revised: *January 13, 2017*
Accepted: *March 13, 2017*
Published: *April 14, 2017*

Measurement of the inclusive cross-sections of single top-quark and top-antiquark t-channel production in pp collisions at $\sqrt{s}$ = 13 TeV with the ATLAS detector

The ATLAS collaboration

E-mail: atlas.publications@cern.ch

Abstract: A measurement of the t-channel single-top-quark and single-top-antiquark production cross-sections in the lepton+jets channel is presented, using 3.2 fb^{-1} of proton-proton collision data at a centre-of-mass energy of 13 TeV, recorded with the ATLAS detector at the LHC in 2015. Events are selected by requiring one charged lepton (electron or muon), missing transverse momentum, and two jets with high transverse momentum, exactly one of which is required to be b-tagged. Using a binned maximum-likelihood fit to the discriminant distribution of a neural network, the cross-sections are determined to be $\sigma(tq) = 156 \pm 5\,(\text{stat.}) \pm 27\,(\text{syst.}) \pm 3\,(\text{lumi.})$ pb for single top-quark production and $\sigma(\bar{t}q) = 91 \pm 4\,(\text{stat.}) \pm 18\,(\text{syst.}) \pm 2\,(\text{lumi.})$ pb for single top-antiquark production, assuming a top-quark mass of 172.5 GeV. The cross-section ratio is measured to be $R_t = \sigma(tq)/\sigma(\bar{t}q) = 1.72 \pm 0.09\,(\text{stat.}) \pm 0.18\,(\text{syst.})$. All results are in agreement with Standard Model predictions.

Keywords: Hadron-Hadron scattering (experiments)

ArXiv ePrint: 1609.03920

doi:10.1007/JHEP04(2017)086

JHEP04(2017)086

Contents

JHEP04(2017)086

1 Introduction

After its restart in 2015, the Large Hadron Collider (LHC) [1] has been producing proton-proton (pp) collisions at a centre-of-mass energy of $\sqrt{s} = 13\,\text{TeV}$, giving the collider experiments access to a so far unexplored kinematic range. It is important to measure all accessible Standard Model (SM) processes at the new centre-of-mass energy, compare the results to the corresponding theoretical SM predictions, and look for deviations which might result from energy-dependent non-SM couplings. In this article, inclusive cross-section measurements of the dominant single-top-quark production mechanism are presented.

At leading order (LO) in perturbation theory, single top-quark production is described by three subprocesses that are distinguished by the virtuality of the exchanged W boson. The dominant process is the t-channel exchange depicted in figure 1, which is the subject of the measurements presented in this article. A light quark from one of the colliding protons interacts with a b-quark from another proton by exchanging a virtual W boson. Since the valence u-quark density of the proton is about twice as high as the valence d-quark density, the production cross-section of single top-quarks $\sigma(tq)$ is expected to be higher than the cross-section of top-antiquark production $\sigma(\bar{t}q)$. At LO, the subleading single-top-quark processes are the associated production of a W boson and a top quark (Wt) and the s-channel production of $t\bar{b}$ and $\bar{t}b$.

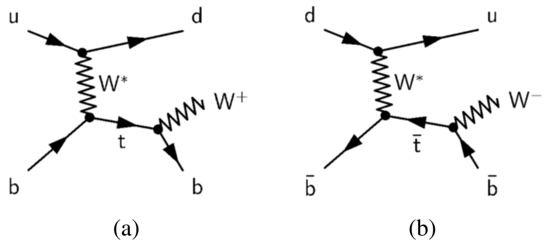

Figure 1. Representative leading-order Feynman diagrams of (a) single-top-quark production and (b) single-top-antiquark production via the t-channel exchange of a virtual W boson (W^*), including the decay of the top quark and top antiquark, respectively.

In this article, measurements of $\sigma(tq)$ and $\sigma(\bar{t}q)$ in proton-proton collisions at a centre-of-mass energy of $\sqrt{s} = 13$ TeV are presented. The analysis is based on the ATLAS data set collected in 2015 corresponding to an integrated luminosity of 3.2 fb^{-1}. Separate measurements of tq and $\bar{t}q$ production provide sensitivity to the parton distribution functions (PDFs) of the u-quark and the d-quark [2], exploiting the different initial states of the two processes as shown in figure 1. In addition, the cross-section ratio $R_t \equiv \sigma(tq)/\sigma(\bar{t}q)$ is measured, featuring smaller systematic uncertainties than the individual cross-sections because of partial cancellations of common uncertainties.

In general, measurements of single top-quark production provide insights into the properties of the Wtb vertex. The cross-sections are proportional to the square of the coupling at the production vertex. In the SM, the coupling is given by the Cabibbo-Kobayashi-Maskawa (CKM) matrix element V_{tb} [3, 4] multiplied by the universal electroweak coupling constant. Non-SM contributions can be encapsulated by an additional left-handed form factor $f_{\rm LV}$ [5], assumed to be real. The sensitivity for these non-SM contributions could be increased for the higher centre-of-mass energy, if there is new physics at high scales. The combined cross-section $\sigma(tq + \bar{t}q)$ is determined as the sum of $\sigma(tq)$ and $\sigma(\bar{t}q)$ and used to determine $f_{\rm LV} \cdot |V_{tb}|$. All measurements presented in this paper are based on the assumption that the production and the decay of top quarks via Wts and Wtd vertices is suppressed due to the fact that the CKM matrix elements V_{ts} and V_{td} are much smaller than V_{tb}. Currently, the most precise determination of $f_{\rm LV} \cdot |V_{tb}|$ has an uncertainty of 4 %, obtained from a combination of measurements performed by the CMS Collaboration [6] under the same assumption as the one stated above.

In pp collisions at $\sqrt{s} = 13$ TeV, the predicted production cross-section of the t-channel single-top-quark process is $\sigma(tq) = 136.0^{+5.4}_{-4.6}$ pb for top-quark production and $\sigma(\bar{t}q) = 81.0^{+4.1}_{-3.6}$ pb for top-antiquark production. These predictions have been calculated for a top-quark mass of 172.5 GeV at next-to-leading order (NLO) [7] in perturbative QCD using Hathor v2.1 [8]. The uncertainties connected with PDFs and the strong coupling constant, $\alpha_{\rm s}$, are calculated using the PDF4LHC prescription [9] with the MSTW2008 NLO [10, 11], CT10 NLO [12] and NNPDF 2.3 NLO [13] PDF sets, and are added in quadrature to the scale uncertainty. The cross-sections of all three single-top-quark production processes have also been calculated at approximate next-to-next-to-leading-order (NNLO) precision [14–16]. NNLO results are available for the t-channel cross-section [17] and the NNLO/NLO K-factor is 0.985. However, the NLO calculation of this process features a more comprehensive uncertainty treatment, including a complete treatment of the PDF and scale uncertainties, compared to the NNLO one, and is therefore used to extract $f_{\rm LV} \cdot |V_{tb}|$.

JHEP04(2017)086

In this analysis, the event selection targets tq and $\bar{t}q$ events with leptonically decaying W bosons. The lepton is either an electron or a muon, where events involving $W \to \tau\nu$ decays with a subsequent decay of the τ lepton to $e\nu_e\nu_\tau$ or $\mu\nu_\mu\nu_\tau$ are included in the signal. The experimental signature of selected events is thus given by one prompt isolated electron or muon, missing transverse momentum, $E_{\mathrm{T}}^{\mathrm{miss}}$, and two hadronic jets with high transverse momentum, p_{T},[1] where one of these jets originates from a b-quark (b-jet) and the second one is produced primarily in the forward direction. The presence of additional jets is vetoed to suppress background from $t\bar{t}$ production.

Several other processes feature the same signature as single-top-quark events; the main backgrounds are W+jets production and top-quark-antiquark ($t\bar{t}$) pair production. In order to improve the sensitivity of the signal extraction, an artificial neural network (NN) [18] is used to discriminate between signal and background events, following the same strategy that was used in comprehensive measurements of t-channel single top-quark production at $\sqrt{s}$ =7 TeV [19].

This article is organised as follows. Section 2 gives an overview of the data and simulated event samples that are used in the analysis. The definitions of physics objects are given in section 3 and the event selection criteria as well as the definition of the signal and validation regions are presented in section 4. Section 5 describes the estimation of the background processes and compares the predicted kinematic distributions to data. Section 6 discusses the discriminating variables and the training and the performance of the NN used to improve the measurement sensitivity, while in section 7 the estimation of systematic uncertainties is discussed. Section 8 is devoted to the statistical analysis and section 9 to the measurement of the signal cross-sections and their ratio, and the extraction of $f_{\mathrm{LV}} \cdot |V_{tb}|$. Finally, the conclusion is given in section 10.

2 Data and simulation samples

The ATLAS experiment [20] at the LHC is a multi-purpose particle detector with a forward-backward symmetric cylindrical geometry and a near 4π coverage in solid angle. It consists of an inner tracking detector surrounded by a thin superconducting solenoid providing a 2 T axial magnetic field, electromagnetic and hadron calorimeters, and a muon spectrometer. The inner tracking detector (ID) covers the pseudorapidity range $|\eta| < 2.5$. It consists of silicon pixel, silicon microstrip, and transition-radiation tracking detectors. The innermost layer of the pixel detector, the insertable B-layer [21], was added between Run 1 (2009-2013) and Run 2 of the LHC at a radius of 33 mm around a new and thinner beam pipe. Lead/liquid-argon (LAr) sampling calorimeters provide electromagnetic (EM) energy measurements with high granularity. A hadron (iron/scintillator-tile) calorimeter covers the central pseudorapidity range ($|\eta| < 1.7$). The endcap and forward regions are instrumented with LAr calorimeters for both the EM and hadronic energy measurements up to $|\eta| = 4.9$. The muon spectrometer surrounds the calorimeters and is based on three large air-core toroid superconducting magnets with eight coils each. Its bending power ranges from 2.0 to 7.5 T m. It includes a system of precision tracking chambers and fast detectors

[1] ATLAS uses a right-handed coordinate system with its origin at the nominal interaction point in the centre of the detector and the z-axis is along the beam direction; the x-axis points towards the centre of the LHC ring and the y-axis points upwards. The pseudorapidity η is defined as $\eta = -\ln[\tan(\theta/2)]$, where the polar angle θ is measured with respect to the z-axis. The azimuthal angle, ϕ, is measured with respect to the x-axis. Transverse momentum and energy are defined as $p_{\mathrm{T}} = p\sin\theta$ and $E_{\mathrm{T}} = E\sin\theta$, respectively. The ΔR distance in (η,ϕ) space is defined as $\Delta R = \sqrt{(\Delta\eta)^2 + (\Delta\phi)^2}$.

JHEP04(2017)086

for triggering. A two-level trigger system [22] is used to select events. The first-level trigger is implemented in hardware and uses a subset of the detector information to reduce the accepted rate to at most 75 kHz. This is followed by a software-based high-level trigger (HLT), which has access to full detector granularity and is used to further reduce the event rate to 1 kHz.

This analysis is performed using pp collision data recorded at a centre-of-mass energy of $\sqrt{s}$ = 13 TeV with the ATLAS detector in 2015 in the periods when the LHC was operating with 25 ns bunch spacing. Only the periods in which all the subdetectors were operational are considered, resulting in a data sample with a total integrated luminosity of $\mathcal{L} = 3.2\,\text{fb}^{-1}$.

All generated samples are passed through the simulation of the ATLAS detector [23] based on Geant4 [24]. The same offline reconstruction methods used with data events are applied to the simulated events samples. Minimum-bias events generated by Pythia 8 [25] are used to simulate multiple pp interactions in the same and nearby bunch crossings (pile-up). The simulated pile-up events are reweighted to reproduce the luminosity spectrum in the data.

Electroweak t-channel single-top-quark production can be simulated in different schemes concerning the treatment of the initial b-quark. In the five-flavour scheme (5FS) the b-quarks are treated massless and the LO Feynman diagram is represented by the $2 \to 2$ process with a b quark in the initial state, depicted in figure 1. In the four-flavour scheme (4FS), the PDFs only contain parton distributions for the quarks lighter than the b-quark and therefore the LO Feynman diagram is represented by a $2 \to 3$ process including the $g \to b\bar{b}$ splitting in the initial state. In this scheme, the b-quarks are treated massive.

Signal t-channel single-top-quark events are generated in the 4FS using the Powheg-Box V1 (r2556) [26, 27] generator Events are generated with the fixed four-flavour PDF set CT10f4 [12] and the renormalisation and factorisation scales, μ_r, and, μ_f, are set following the recommendation given in ref. [26]. Top quarks are decayed at LO using MadSpin to preserve all spin correlations. The parton shower, hadronisation, and the underlying event are modelled using the Pythia 6 (v6.428) [28] generator and the Perugia2012 set of tuned parameters (P2012 tune) [29]. In order to study effects of the choice of parton-shower model, the same events are showered using Herwig++ (v.2.7.1) [30] and the energy-extrapolated underlying event set of tuned parameters (UE-EE-5 tune) [31]. A second NLO generator capable of generating t-channel single-top-quark events in the 4FS is MadGraph5_aMC@NLO [32] (v2.2.2). Samples are generated using the CT10f4 PDF set and μ_r and μ_f are set to be the same as those implemented in Powheg-Box. Again, the top quarks produced in the ME are decayed using MadSpin to preserve all spin correlations. The events are showered using Herwig++ (v.2.7.1) and the UE-EE-5 tune. For the generation of SM single top-quarks in the Wt and the s-channel ($t\bar{b} + \bar{t}b$) the Powheg-Box V1 (r2819) generator [33, 34] with the CT10 PDF set is used. Samples of $t\bar{t}$ events are generated with the Powheg-Box V2 (r3026) [35] and the CT10 PDF set. The h_damp parameter, which controls the p_T of the first additional emission beyond the Born configuration, where its main effect is to regulate the high-p_T emission against which the $t\bar{t}$ system recoils, is set to the top-quark mass. The parton shower, hadronisation, and the underlying event are added using Pythia 6 and the P2012 tune.

All top-quark processes are generated assuming a top-quark mass of 172.5 GeV. The top quark is set to decay exclusively to $t \to Wb$, and the EvtGen v1.2.0 program [36] is used to model bottom- and charm-hadron decays.

To model the W+jets and Z+jets background, the SHERPA v2.2.0 [37] generator is used. Matrix elements are calculated for up to two partons at NLO and up to four partons at LO using the Comix [38] and OpenLoops [39] ME generators and merged with the SHERPA parton shower [40] using the ME+PS@NLO prescription [41]. The NNPDF 3.0 PDF set [42] is used in conjunction with dedicated parton-shower tuning developed by the SHERPA authors.

Diboson events, denoted VV, are also simulated using the SHERPA v2.1.1 generator. Matrix elements contain all diagrams with four electroweak vertices. They are calculated for zero partons at NLO and up to three partons at LO using the same methodology as for W/Z+jets production. The CT10 PDF set is used in conjunction with dedicated parton-shower tuning developed by the SHERPA authors.

The only background for which no simulated events are used is the multijet background. Multijet events may be selected if a jet is misidentified as an isolated lepton (”fake” lepton) or if a non-prompt lepton from a hadronic decay appears to be isolated. In the electron channel, the matrix method is used, while in the muon channel, the so-called ‘anti-muon’ method is employed to estimate the multijet background [43]. More details are given in section 5.

3 Object reconstruction

In this section, the reconstruction and selection of electrons, muons, jets and $E_{\mathrm{T}}^{\mathrm{miss}}$ is described.

Electron candidates are defined as clusters of energy deposits in the electromagnetic calorimeter associated with a well-measured track fulfilling several quality requirements [44, 45]. They are required to satisfy $p_{\mathrm{T}} > 30\,\mathrm{GeV}$ and $|\eta_{\mathrm{clus}}| < 2.47$, where η_{clus} is the pseudorapidity of the cluster of energy deposits in the calorimeter. Electron candidates in the calorimeter barrel-endcap transition region $1.37 < |\eta_{\mathrm{clus}}| < 1.52$ are excluded. Isolation criteria are applied to reduce background events, in which a hadronic jet is misidentified as a prompt electron or electrons from the decay of heavy quarks. The criteria are optimised such that by adjusting the isolation threshold the selection efficiency of the isolation criteria is uniform across η. It increases from 90 % for $p_{\mathrm{T}} = 25\,\mathrm{GeV}$ to 99 % for $p_{\mathrm{T}} = 60\,\mathrm{GeV}$. The p_{T} of all tracks within a cone of size $\Delta R = \sqrt{(\Delta\eta)^2 + (\Delta\phi)^2} = 0.3$ around the electron direction, excluding the track belonging to the electron candidate (track isolation), is restricted to be below a threshold depending on the electron p_{T}. In addition, calorimeter isolation in a cone size of 0.2 around the electron is required [46].

Muon candidates are reconstructed by matching track segments or complete tracks in the muon spectrometer with inner detector tracks. The candidates are required to have a transverse momentum $p_{\mathrm{T}} > 25\,\mathrm{GeV}$ and to be in the pseudorapidity region $|\eta| < 2.5$. Additional requirements on the transverse impact parameter significance of $|d_0/\sigma_{d_0}| < 3$ and on the longitudinal impact parameter (z_0) of $|\Delta z_0 \sin\theta| < 0.5\,\mathrm{mm}$ are imposed. Isolation criteria similar to those for electron candidates are imposed.

Jets are reconstructed using the anti-k_t algorithm [47] with a radius parameter of 0.4. They are calibrated using a combination of an energy- and η-dependent simulation-based scheme and a scheme based on data [48]. Only jets with $p_{\mathrm{T}} > 30\,\mathrm{GeV}$ and $|\eta| < 3.5$ are accepted. The rapidity range is determined using a W+jets-dominated validation region and defined by requiring good agreement between simulated and measured data.

JHEP04(2017)086

If any jet is close to an electron, with $\Delta R < 0.2$, the closest jet is removed, as in these cases the jet and the electron are very likely to correspond to the same physical object. Remaining electron candidates overlapping with jets within $\Delta R < 0.4$ are subsequently rejected. To reduce contributions from muons which stem from heavy-flavour decays inside a jet, muons are removed if they are separated from the nearest jet by $\Delta R < 0.4$. However, jets with fewer than three tracks and separated from a muon by $\Delta R < 0.4$ are removed to reduce fake jets from muons depositing a large fraction of their energy in the calorimeters.

To discriminate between jets from the hard-scatter process and those from pile-up, a discriminant called the jet vertex tagger (JVT) [49] is constructed from tracking and vertexing information using a two-dimensional likelihood method. The JVT variable is required to be larger than 0.64 for the jets with $p_T < 50$ GeV and $|\eta| < 2.4$, corresponding to 92 % efficiency and 2 % misidentification rate.

In this analysis, a b-tagging algorithm based on boosted decision trees which is optimised to reject c-quark jets as well as light-quark jets is used. The b- and c-tagging efficiencies, and the mistag rate for the taggers, are measured using the methods described in refs. [50, 51]. The b-tagging algorithm has an efficiency of about 60 % for b-jets in simulated $t\bar{t}$ events, while 0.06 % of light-quark jets and 4.7 % of c-quark jets are mistagged as b-quark jets. The algorithm can only be applied to jets within the coverage of the ID, i.e. $|\eta| < 2.5$.

The magnitude of the missing transverse momentum vector is defined as $E_T^{miss} = |\vec{E}_T^{miss}|$, where $\vec{E}_T^{miss}$ is calculated using the calibrated three-dimensional calorimeter energy clusters associated with the selected jets together with either the calibrated calorimeter energy cluster associated with an electron or the p_T of a muon track (hard components). Contributions from soft particles, not associated with these identified particles, are accounted for using tracks associated to the vertex but not associated with a jet, electron, or muon (soft components).

4 Event selection

Events are considered only if they are accepted by at least one of two single-muon or single-electron triggers [52]. Events in the electron channel are triggered by a calorimeter cluster matched to a track, and the trigger electron object is required to have either $E_T > 60$ GeV or $E_T > 24$ GeV and satisfy isolation criteria. Events in the muon channel are triggered by either requiring an isolated muon with $p_T > 20$ GeV or requiring a muon with $p_T > 50$ GeV.

Only events containing exactly one isolated charged lepton (electron or muon) with $p_T > 30$ GeV and $|\eta| < 2.5$ are accepted. Candidate events must have exactly two jets satisfying the criteria described in section 3. Jets reconstructed in the range $2.75 < |\eta| < 3.5$, covering the endcap-forward calorimeter transition region, must have $p_T > 35$ GeV. At least one of the selected jets is required to be identified (b-tagged) as a b-jet.

In order to reduce the number of multijet background events, which are characterised by low E_T^{miss} and low W-boson transverse mass[2] $m_T(\ell E_T^{miss})$, the event selection requires $E_T^{miss} > 30$ GeV and $m_T(\ell E_T^{miss}) > 50$ GeV. To further suppress the multijet background a requirement on the p_T of

[2]The W-boson transverse mass is defined as: $m_T(\ell E_T^{miss}) = \sqrt{2\left[p_T(\ell)E_T^{miss} - \vec{p}_T(\ell)\cdot\vec{E}_T^{miss}\right]}$, where $\vec{p}_T(\ell)$ denotes the transverse momentum of the electron or muon and $p_T(\ell)$ its modulus.

the charged lepton and the azimuthal angle between the charged lepton and jet is applied:

$$p_T(\ell) > \max\left(30\,\text{GeV}, 40\,\text{GeV}\cdot\frac{|\Delta\phi(j_1,\ell)|}{\pi}\right), \tag{4.1}$$

where ℓ denotes the identified charged lepton and j_1 the reconstructed jet with the highest p_T.

Contributions from processes with two isolated leptons in the final state are suppressed by rejecting any event with an additional electron or muon as defined above satisfying $p_T > 10$ GeV.

Three kinematic regions are defined in this analysis, all three being subject to the same event selection requiring one electron or muon, missing transverse momentum and one or two b-tagged jets:

- The signal region (SR) is defined by using the default b-tagging requirement and selecting exactly one b-tagged jet.
- The W-boson validation region (W+jets VR) requires exactly one b-tagged jet, but with a less stringent b-tagging requirement with a b-tagging efficiency of 85 %. Events contained in the SR are rejected. The validation region is defined such, that the composition of the resulting sample is dominated by W+jets production with a purity of 77 % and the same reconstruction of the top-quark kinematics can be used as in the signal region, in order to check the modelling of kinematic variables.
- Events in the $t\bar{t}$ validation region ($t\bar{t}$ VR) are required to have exactly three jets of which exactly two are b-tagged jets using the default b-tagging requirement. This validation region is highly enriched in $t\bar{t}$ events with a purity of 85 %.

5 Background estimation

For all background processes, except the multijet background, the number of expected events are obtained from Monte Carlo (MC) simulation scaled to the theoretical cross-section predictions. The associated production of an on-shell W boson and a top quark (Wt) has a predicted production cross-section of 71.1 pb [15] calculated at approximate NNLO accuracy. Predictions of the s-channel production are calculated at NLO using the same methodology as for the t-channel production and yield a cross-section of 10.3 pb. The predicted $t\bar{t}$ cross-section is $\sigma_{t\bar{t}} = 831.8$ pb. It has been calculated at NNLO in QCD including resummation of next-to-next-to-leading logarithmic (NNLL) soft gluon terms with top++2.0 [53–58]. All quoted cross-sections are given for $m_{\text{top}} = 172.5$ GeV. The inclusive cross-sections of W+jets and Z+jets production are calculated at NNLO with FEWZ [59]. Diboson events are normalised to the NLO cross-section provided by the Sherpa generator.

The matrix method [43] is used to determine the multijet background in the electron channel. This method estimates the number of multijet background events in the signal region by applying efficiency factors to the number of events passing the signal tight and a loose lepton selection, the former selection being a subset of the latter. The number of multijet events $N^{\text{tight}}_{\text{fake}}$ passing the signal requirements can be expressed as

$$N^{\text{tight}}_{\text{fake}} = \frac{\epsilon_{\text{fake}}}{\epsilon_{\text{real}} - \epsilon_{\text{fake}}}\cdot\left(N^{\text{loose}}\epsilon_{\text{real}} - N^{\text{tight}}\right), \tag{5.1}$$

where ϵ_{real} and ϵ_{fake} are the efficiencies for real and fake loose leptons being selected as tight leptons, N^{loose} is the number of selected events in the loose sample, and N^{tight} is the number of selected events in the signal sample. The fake-lepton efficiencies are determined from a data sample dominated by non-prompt and fake-lepton background events. This sample is selected by requiring exactly one loose lepton and low $E_{\mathrm{T}}^{\mathrm{miss}}$ as well as low $m_{\mathrm{T}}(\ell E_{\mathrm{T}}^{\mathrm{miss}})$. The real-lepton efficiencies are also estimated from collision data using a "tag-and-probe" method in $Z \to ee$ events.

Multijet-background events containing non-prompt muons are modelled with a sample of events enriched in non-isolated muons [43]. Most of these events originate from b-hadron or c-hadron decays in jets. These events pass the same kinematic requirements as the events of the signal sample. Only some of the muon identification cuts are modified, ensuring that there is no overlap with the signal selection. The normalisation is determined using a binned maximum-likelihood fit.

The fit is performed to the observed data in the $m_{\mathrm{T}}(\ell E_{\mathrm{T}}^{\mathrm{miss}})$ distribution after applying all selection criteria, except the requirement on $m_{\mathrm{T}}(\ell E_{\mathrm{T}}^{\mathrm{miss}})$. The multijet template is fit together with templates derived from MC simulation for all other processes. The rate uncertainties are accounted for in the fitting process in the form of additional constrained nuisance parameters. For the purpose of this fit, three different template distributions are used. One template is built from simulated W+jets events, one consists of events from $t\bar{t}$ and single top-quark production, and one consists of contributions from Z+jets and VV production. As the shape of the joint template of Z+jets and VV events is very similar to that of W+jets events, the rates are fixed in the fitting process.

The estimated event rates obtained from the binned maximum-likelihood fit for the combined contributions of W+jets, $t\bar{t}$ and single top-quark production are not used in the later analysis and are only applied to scale the respective processes in order to check the modelling of the kinematic distributions. For the neural-network training, as well as for the final statistical analysis, the normalisation for all but the multijet background is taken from MC simulations scaled to their respective cross-section predictions.

In the signal region, 34459 events in the ℓ^{+} channel and 31056 events in the ℓ^{-} channel are observed in data, while the expected SM background amounts to 33600 ± 2600 events and 30200 ± 2300 events, respectively. The quoted uncertainties are statistical uncertainties and the uncertainty in the number of multijet events. Table 1 summarises the event yields in the signal region for each of the background processes considered together with the event yields for the signal process. The yields are calculated using the acceptance from MC samples normalised to their respective theoretical cross-sections including the (N)NLO K factors.

In the following, the electron and muon channel are combined for all figures and fits. Different processes are also grouped together in the following way. The top-quark background consists of all background processes that include the production of top quarks. These processes are $t\bar{t}$ production and single top-quark production in the Wt and $t\bar{b}$+$\bar{t}b$ channel. The W+jets process describes the production of a real W boson in association with jets, while the production of a Z boson or two vector bosons VV in association with jets are grouped together to Z, VV+jets. Finally, multijets represents events with a fake lepton originating from multijet production.

Process	ℓ^+ channel	ℓ^- channel
tq	$4\,200 \pm 170$	8 ± 3
$\bar{t}q$	5 ± 2	$2\,710 \pm 140$
$t\bar{t}$	$13\,100 \pm 790$	$13\,100 \pm 790$
Wt	$1\,640 \pm 110$	$1\,640 \pm 110$
$t\bar{b}$+$\bar{t}b$	298 ± 25	199 ± 18
W^++jets	$10\,500 \pm 2\,200$	< 1
W^-+jets	< 1	$8\,730 \pm 1\,800$
Z, VV+jets	$1\,530 \pm 320$	$1\,410 \pm 300$
Multijets	$2\,400 \pm 1\,200$	$2\,400 \pm 1\,200$
Total expected	$33\,600 \pm 2\,600$	$30\,200 \pm 2\,300$
Data observed	34 459	31 056

Table 1. Predicted and observed event yields for the signal region. The quoted uncertainties include uncertainties in the theoretical cross-sections, in the number of multijet events, and the statistical uncertainties.

6 Discrimination of signal and background events

To separate t-channel single-top-quark signal events from the background, several kinematic variables are combined into one discriminant by employing a neural network [18, 60]. A large number of potential input variables were studied, including kinematic variables of the identified physics objects, as well as variables obtained from the reconstruction of the W boson and the top quark. A detailed description of the algorithm including the reconstruction of the longitudinal component of the neutrino momentum is given in ref. [19]. As a compromise between the discrimination power and the need for a manageable number of variables, the ten highest-ranking variables are chosen and are listed in table 2. The two most discriminating variables are the reconstructed top-quark mass $m(\ell\nu b)$ and the invariant mass of the two jets $m(jb)$. Figures 2(a) and 2(b) show the $m(l\nu b)$ and $m(jb)$ distributions (normalised to unit area) in the SR for the ℓ^+ channel. Figures 2(c)–2(f) show the $m(l\nu b)$ and $m(jb)$ distributions in the W+jets VR and $t\bar{t}$ VR for the ℓ^+ channel. In the $t\bar{t}$ VR the b-jet used to calculate $m(l\nu b)$ and $m(jb)$ is the b-jet with the higher p_{T}. The distributions from the different processes, apart from the multijet background in the electron channel, are normalised to match the number of observed events. In the case of the electron channel, the relative contribution of each simulated process is estimated using its predicted cross-section. In the case of the muon channel, the distributions are normalised to the expected number of events obtained from the fit to the $m_{\mathrm{T}}(\ell E_{\mathrm{T}}^{\mathrm{miss}})$ distributions described in section 5. Satisfactory agreement is seen between the data and the predictions.

The NN infrastructure consists of one input node for each input variable plus one bias node, an arbitrary user-defined number of hidden nodes, and one output node which gives a continuous output in the interval [0, 1]. In this specific case, 15 nodes in the hidden layer are used and equal numbers of signal and background events were used in the training, where the different background processes are weighted according to their expected number of events. The shapes of the resulting NN discriminant distributions (O_{NN}) for the signal and the two largest backgrounds are shown in figure 3 together with the data distributions compared to the predictions in the two validation regions. Good agreement between the predicted and observed distributions is found.

JHEP04(2017)086

Variable	Definition
$m(\ell\nu b)$	top-quark mass reconstructed from the charged lepton, neutrino, and b-tagged jet
$m(jb)$	invariant mass of the b-tagged and untagged jet
$m_{\mathrm{T}}(\ell E_{\mathrm{T}}^{\mathrm{miss}})$	transverse mass of the reconstructed W boson
$\lvert\eta(j)\rvert$	modulus of the pseudorapidity of the untagged jet
$m(\ell b)$	invariant mass of the charged lepton (ℓ) and the b-tagged jet
$\eta(\ell\nu)$	rapidity of the reconstructed W boson
$\Delta R(\ell\nu b, j)$	ΔR of the reconstructed top quark and the untagged jet
$\cos\theta^{*}(\ell, j)$	cosine of the angle θ^{*} between the charged lepton and the untagged jet in the rest frame of the reconstructed top quark
$\Delta p_{\mathrm{T}}(\ell\nu b, j)$	Δp_{T} of the reconstructed top quark and the untagged jet
$\Delta R(\ell, j)$	ΔR of the charged lepton and the untagged jet

Table 2. The ten variables that are used in the training of the neural network ordered by their discriminating power as determined by Neurobayes [19, 60].

7 Systematic uncertainties

Systematic uncertainties in the normalisation of the individual backgrounds and in the signal acceptance as well as uncertainties in the shape of the NN discriminant distribution of the individual predictions affect the individual top-quark and top-antiquark cross-section measurements and their ratio. The uncertainties are split into the following categories.

Reconstruction efficiency and calibration uncertainties. Systematic uncertainties affecting the reconstruction and energy calibration of jets, electrons, and muons are propagated through the analysis. The dominant source for this measurement arises from the jet energy scale (JES) calibration, including the modelling of pile-up, and from the b-jet tagging efficiencies.

The uncertainties due to lepton reconstruction, identification and trigger efficiencies are estimated using tag-and-probe methods in $Z \to \ell\ell$ events. Correction factors are derived to match the simulation to observed distributions in collision data and associated uncertainties are estimated. To estimate uncertainties in the lepton momentum scale and resolution, also $Z \to \ell\ell$ events are used [61–63]. The lepton-charge misidentification is estimated with simulated events and found to be below 0.1 %, see table 1. The uncertainty on the lepton-charge misidentification is evaluated and found to be negligible.

Several components of the JES uncertainty are considered [64, 65]. Uncertainties derived from different dijet-p_{T}-balance measurements as well as uncertainties associated with in-situ calibration techniques are considered. Furthermore, the presence of nearby jets and the modelling of pile-up affects the jet calibration. The uncertainty in the flavour composition covers effects due to the difference in quark-gluon composition between the jets used in the calibration and the jets used in this analysis. Also an uncertainty due to limited knowledge of the calorimeter response to light-quark jets and gluon jets is considered. Finally, the JES uncertainty is estimated for b-quark jets by varying the modelling of b-quark fragmentation. The uncertainty in the jet energy resolution is modelled by varying the p_{T} of the jets according to the systematic uncertainties of the

JHEP04(2017)086

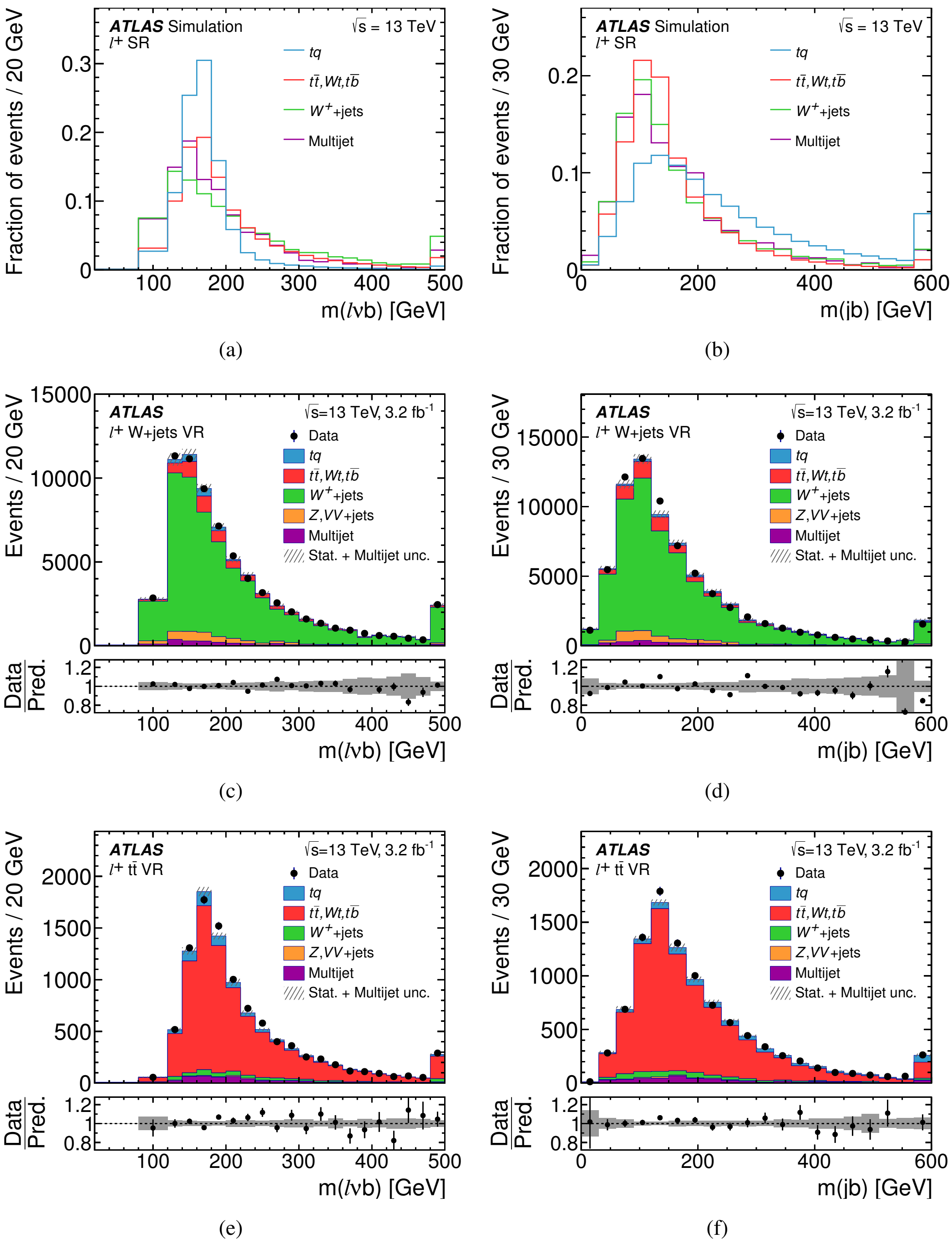

Figure 2. Distributions of the two most discriminating variables, (left) the reconstructed top-quark mass $m(\ell\nu b)$ and (right) the invariant mass of the jet pair $m(jb)$, for the ℓ^+ channel. In the $t\bar{t}$ VR the b-jet used to calculate $m(l\nu b)$ and $m(jb)$ is the b-jet with the higher p_{T}. (a)-(b): signal and background distributions normalised to unit area. (c)-(f): observed distributions in the W+jets VR and the $t\bar{t}$ VR compared to the model obtained from simulated events. The simulated distributions are normalised to match the number of observed events as described in the main text. The hatched and grey error bands represent the uncertainty in the number of multijet events and the uncertainty due to the size of the MC samples. The ratio of observed to predicted (Pred.) number of events in each bin is shown in the lower distributions. Events in the overflow are contained in the last bin.

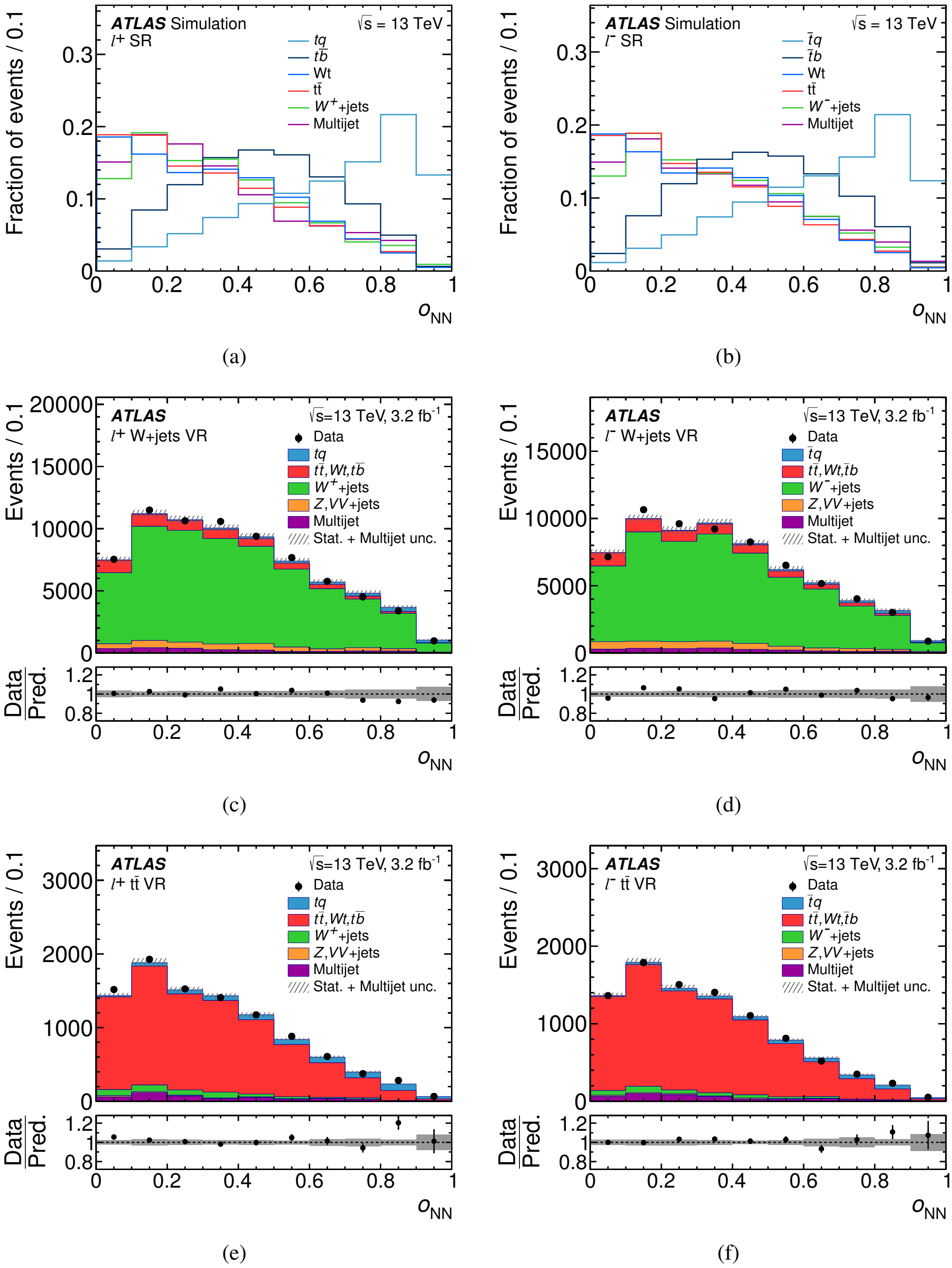

Figure 3. Distributions of the NN discriminant O_{NN} (left) for the ℓ^+ channel and (right) for the ℓ^- channel. (a)-(b): signal and background distributions normalised to unit area. (c)-(f): observed distributions in the W+jets VR and the $t\bar{t}$ VR compared to the model obtained from simulated events. The simulated distributions are normalised to match the number of observed events as described in the main text. The hatched and grey error bands represent the uncertainty in the number of multijet events and the uncertainty due to the size of the MC samples. The ratio of observed to predicted (Pred.) number of events in each bin is shown in the lower distributions.

resolution measurement [66]. The effect of uncertainties associated with the JVT requirement is also considered.

The impact of a possible miscalibration on the soft track component of $E_{\mathrm{T}}^{\mathrm{miss}}$ is derived from data-MC comparisons of the p_{T} balance between the hard and soft $E_{\mathrm{T}}^{\mathrm{miss}}$ components.

Since the analysis makes use of b-tagging, the uncertainties in the b- and c-tagging efficiencies and the mistag rate are taken into account. These uncertainties were determined using $\sqrt{s} = 8$ TeV data as described in ref. [51] for b-jets and ref. [50] for c-jets and light jets, with additional uncertainties to account for the presence of the newly added Insertable B-Layer and the extrapolation to $\sqrt{s} = 13$ TeV.

Monte Carlo generators. Systematic effects from MC modelling of the signal and the $t\bar{t}$ background process are either estimated by comparing different generators or by comparing parameter variations in the Powheg-Box + Pythia 6 setup. The Powheg-Box + Herwig++ sample is used for parton shower and hadronisation modelling studies, while MadGraph5_aMC@NLO + Herwig++ is used for studies of the NLO-matching method. Variations of the amount of additional radiation are studied by changing μ_{r} and μ_{f} and the scales in the parton shower simultaneously. In these samples, an up-variation of μ_{r} and μ_{f} by a factor of two is combined with the P2012 tune with lower radiation (P2012radLo tune) than the nominal P2012 set, and a variation of both scales by a factor of one half is combined with the P2012 tune with higher radiation (P2012radHi tune). In the case of the up-variation of $t\bar{t}$ production, the h_{damp} parameter is also changed and set to two times the top-quark mass [67].

The uncertainty in the pile-up reweighting as well as the statistical uncertainties of the simulated event samples are also taken into account.

PDF. The systematic uncertainties in the signal and background acceptance related to the parton distribution functions are taken into account for all single-top-quark processes and $t\bar{t}$ production. The procedure follows the updated PDF4LHC recommendation [68] by using the 30 eigenvectors of the PDF4LHC15 NLO PDF set. The events are reweighted according to each of the PDF uncertainty eigenvectors. In addition, the acceptance difference between PDF4LHC15 and CT10 is considered, since the latter PDF set is used in the MC samples and is not covered by the uncertainty obtained with PDF4LHC15 PDF sets.

Background normalisation. The $t\bar{t}$, Wt and $t\bar{b}$ backgrounds are normalised to their theory predictions, where a combined uncertainty of 6 % is derived from the weighted average of the individual uncertainties. The PDF- and α_{s}-induced uncertainties for the $t\bar{t}$ process are calculated using the PDF4LHC prescription [9] with the MSTW2008 68 % CL NNLO, CT10 NNLO and NNPDF PDF sets and added in quadrature to the uncertainty due to the scale, leading to a total uncertainty of 5.5 %. The uncertainty in the Wt cross-section, calculated at approximate NNLO, is the sum in quadrature of the effects of the PDF uncertainty obtained using the MSTW2008 68 % CL NNLO PDF sets and the scale uncertainty, and is found to be 5.4 %. The s-channel production cross-section is calculated at NLO with a total uncertainty of 3.8 %.

For the W+jets and Z+jets backgrounds, an uncertainty of 21 % is assigned. This uncertainty is estimated based on parameter variations in the generation of the Sherpa samples. It was found that correlated variations of the factorisation and renormalisation scales have the biggest impact on the kinematic distributions and produces change covering the unfolded data and their uncertainties [69].

Diboson processes have an uncertainty of 6 % in the inclusive cross-section including uncertainties on the choice of the factorisation and renormalisation scales and the PDF uncertainty.

The multijet background estimate has an uncertainty of 50 %, based on comparisons of the rates obtained using alternative methods described in previous analyses [19, 43, 70].

Luminosity and beam energy. The uncertainty in the integrated luminosity is ±2.1 %. It is derived, following a methodology similar to that detailed in refs. [71] and [72], from a calibration of the luminosity scale using x–y beam-separation scans performed in August 2015. Given the level of precision of the measurement the uncertainty in the beam energy is negligible for this analysis.

All systematic uncertainties discussed above cause variations in the signal acceptance, the background rates and the shape of the NN discriminant distribution. Both the rate and shape uncertainties are taken into account by generating correlated pseudo-experiments as detailed in the next section.

8 Statistical analysis

To extract the top-quark and top-antiquark inclusive cross-sections, a binned maximum-likelihood fit to the NN discriminant distribution is performed in the ℓ^+ channel and ℓ^- channel, treating t-channel top-quark and t-channel top-antiquark production as independent processes. The likelihood function used is built from Poisson probability terms and includes Gaussian priors to constrain the rates of the W+jets and top-quark background processes; more details are given in ref. [19]. The fit parameters of the likelihood function are scale factors, β_i, that multiply the expected value of the number of events, ν_i, for each fitted process i. The background normalisation constraints are 21 % for W+jets production, and 6 % for top-quark backgrounds ($t\bar{t}$, Wt and $t\bar{b} + \bar{t}b$), while the contributions from Z+jets, VV, and multijet processes are fixed to their predictions. The fitted rates of the W+jets background and the top-quark backgrounds are mainly driven by the background-dominated region with low O_{NN} values. The cross-section ratio is subsequently computed as $R_t = \sigma(tq)/\sigma(\bar{t}q)$.

The fit finds the minimum of the negative log-likelihood function for the parameter values shown in table 3. Figure 4 compares the observed NN discriminant distributions to the compound model of signal and backgrounds with each contribution normalised to the fit results from table 3. The three most discriminating variables are presented in figure 5. The model agrees with the data, within uncertainties.

The systematic uncertainties in the cross-section measurements are determined from pseudo-experiments which vary the signal acceptance, the background rates, and the shape of the NN discriminant. By using samples of simulated events with variations reflecting the sources of systematic uncertainty, all of the effects are estimated and the pseudo-experiments are varied accordingly. Rate and shape uncertainties are treated in a correlated way. All systematic uncertainties apart from those related to the Monte Carlo statistics are also treated in a correlated way between the ℓ^+ channel and the ℓ^- channel. Table 4 shows the contributions to the total uncertainty in the inclusive cross-section measurements. The table provides the uncertainties estimated for the observed signal and back-

Process	$\hat{\beta}$	$\hat{\nu}(\ell^+)$	$\hat{\nu}(\ell^-)$
tq	1.15 ± 0.03	$4\,840 \pm 140$	–
$\bar{t}q$	1.12 ± 0.05	–	$3\,040 \pm 130$
$t\bar{t}$, Wt, $t\bar{b} + \bar{t}b$	0.91 ± 0.03	$13\,700 \pm 510$	$13\,600 \pm 510$
W^++ jets	1.13 ± 0.05	$12\,000 \pm 550$	–
W^-+ jets	1.21 ± 0.06	–	$10\,500 \pm 550$
Z, VV+ jets	–	$1\,530$	$1\,410$
Multijet background	–	$2\,420$	$2\,420$
Total estimated	–	$34\,500 \pm 760$	$31\,000 \pm 760$
Total observed	–	$34\,459$	$31\,056$

Table 3. Estimated scale factors, $\hat{\beta}$, and number of events, $\hat{\nu} = \hat{\beta} \cdot \nu$, for the ℓ^+ and ℓ^- channel from the minimisation of the likelihood function. The quoted uncertainties in $\hat{\beta}$ and $\hat{\nu}$ include the statistical uncertainty and the uncertainties from the constraints on the background normalisation as used in the likelihood function.

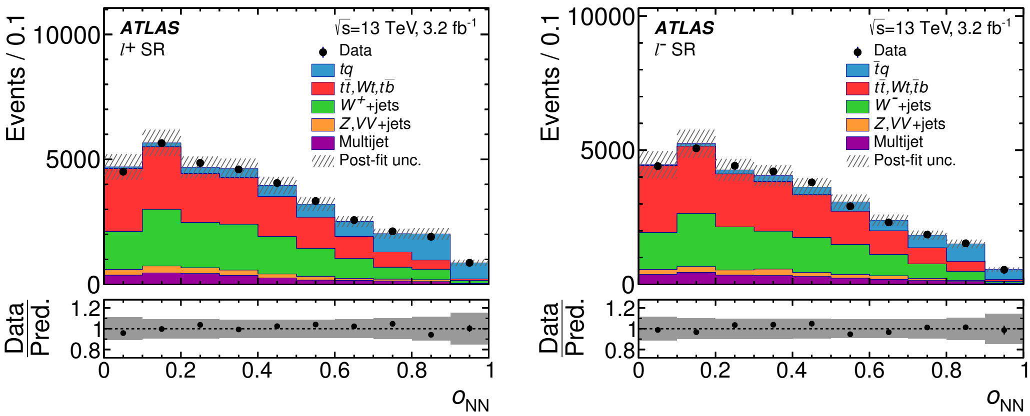

(a) (b)

Figure 4. NN discriminant distribution (a) for the ℓ^+ channel and (b) for the ℓ^- channel in the SR. The signal and backgrounds are normalised to the fit result and the hatched and grey error bands represent the post-fit uncertainty. The ratio of observed to predicted (Pred.) number of events in each bin is shown in the lower histogram.

ground rates as obtained from the maximum-likelihood fit to the observed collision data. Uncertainties in the extrapolation to the full phase space are included in the generator-related uncertainties.

9 Cross-section measurement

After performing the binned maximum-likelihood fit to the NN discriminant distribution and estimating the total uncertainty, the inclusive cross-sections of top-quark and top-antiquark production in the t-channel are measured to be:

$$\sigma(tq) = 156 \pm 5\,(\text{stat.}) \pm 27\,(\text{syst.}) \pm 3\,(\text{lumi.})\ \text{pb}$$
$$\sigma(\bar{t}q) = 91 \pm 4\,(\text{stat.}) \pm 18\,(\text{syst.}) \pm 2\,(\text{lumi.})\ \text{pb}$$
$$R_t = 1.72 \pm 0.09\,(\text{stat.}) \pm 0.18(\text{syst.}),$$

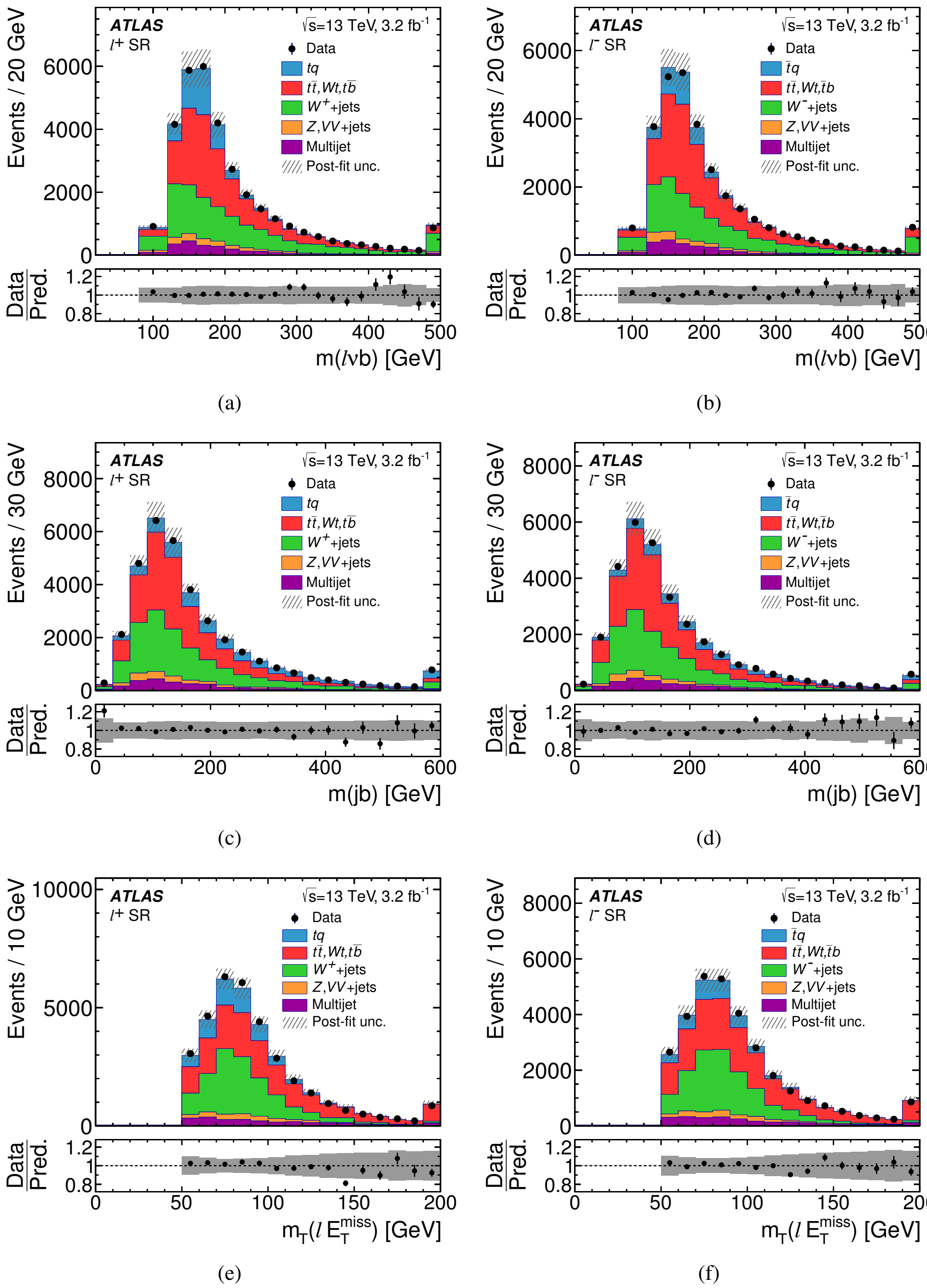

Figure 5. Distributions of the three most important variables (left) for the ℓ^+ channel and (right) for the ℓ^- channel normalised to the fit result. (a)-(b): reconstructed top-quark mass $m(\ell\nu b)$, (c)-(d): invariant mass of the jet pair $m(jb)$, (e)-(f): transverse mass of the W boson $m_{\mathrm{T}}(\ell E_{\mathrm{T}}^{\mathrm{miss}})$. The hatched and grey error bands represents the post-fit uncertainty. The ratio of observed to predicted (Pred.) number of events in each bin is shown in the lower histogram. Events beyond the x-axis range are included in the last bin.

Source	$\frac{\Delta\sigma(tq)}{\sigma(tq)}$ [%]	$\frac{\Delta\sigma(\bar{t}q)}{\sigma(\bar{t}q)}$ [%]	$\frac{\Delta R_t}{R_t}$ [%]
Data statistics	± 2.9	± 4.1	± 5.0
Monte Carlo statistics	± 2.8	± 4.2	± 5.1
Reconstruction efficiency and calibration uncertainties			
Muon uncertainties	± 0.8	± 0.9	± 1.0
Electron uncertainties	< 0.5	± 0.5	± 0.7
JES	± 3.4	± 4.1	± 1.2
Jet energy resolution	± 3.9	± 3.1	± 1.1
$E_{\mathrm{T}}^{\mathrm{miss}}$ modelling	± 0.9	± 1.2	< 0.5
b-tagging efficiency	± 7.0	± 6.9	< 0.5
c-tagging efficiency	< 0.5	± 0.5	± 0.6
Light-jet tagging efficiency	< 0.5	< 0.5	< 0.5
Pile-up reweighting	± 1.5	± 2.2	± 3.8
Monte Carlo generators			
tq parton shower generator	± 13.0	± 14.3	± 1.9
tq NLO matching	± 2.1	± 0.7	± 2.8
tq radiation	± 3.7	± 3.4	± 3.7
$t\bar{t}$, Wt, $t\bar{b}+\bar{t}b$ parton shower generator	± 3.2	± 4.4	± 1.2
$t\bar{t}$, Wt, $t\bar{b}+\bar{t}b$ NLO matching	± 4.4	± 8.6	± 4.6
$t\bar{t}$, Wt, $t\bar{b}+\bar{t}b$ radiation	< 0.5	± 1.1	± 0.7
PDF	± 0.6	± 0.9	< 0.5
Background normalisation			
Multijet normalisation	± 0.3	± 2.0	± 1.8
Other background normalisation	± 0.4	± 0.5	< 0.5
Luminosity	± 2.1	± 2.1	< 0.5
Total systematic uncertainty	± 17.5	± 20.0	± 10.2
Total uncertainty	± 17.8	± 20.4	± 11.4

Table 4. List of systematic uncertainties contributing to the total uncertainty in the measured values of $\sigma(tq)$, $\sigma(\bar{t}q)$, and $R_t = \sigma(tq)/\sigma(\bar{t}q)$. The estimation of the systematic uncertainties has a statistical uncertainty of 0.3 %. Uncertainties contributing less than 0.5 % are marked with "< 0.5".

assuming a top-quark mass of $m_{\mathrm{top}} = 172.5$ GeV. Figure 6 compares the measured value of R_t to NLO predictions [7] obtained with Hathor [8] using different PDF sets. PDF sets are available from various groups worldwide: CTEQ [12, 73], MSTW2008 [10]/MMHT14 [74], NNPDF [42, 75], JR [76], ABM [77], and HERAPDF [78, 79]. Also, the first PDF set provided by the ATLAS Collaboration is considered [80]. The PDFs provided by the different groups differ in the data used, the value of α_{s}, the values of the quark masses, and the treatment of heavy-quark masses. Other differences concern the way higher-order corrections are implemented, the parametrisation of the PDF fitting-model, the way of treating systematic uncertainties and the criteria for estimating con-

JHEP04(2017)086

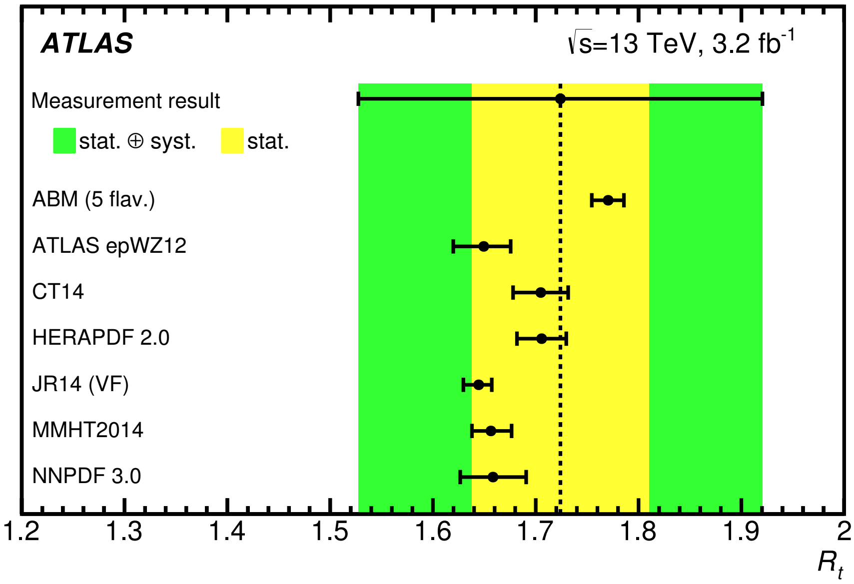

Figure 6. Comparison between observed and predicted values of $R_t = \frac{\sigma_t}{\sigma_{\bar{t}}}$. Predictions are calculated at NLO precision [7, 8] in the five-flavour scheme and given for different NLO PDF sets. The uncertainty includes the uncertainty in the renormalisation and factorisation scales, as well as the combined internal PDF and α_s uncertainty. The dotted black line indicates the measured value. The combined statistical and systematic uncertainty of the measurement is shown in green, while the statistical uncertainty is represented by the yellow error band. Predictions for all presented PDF sets are within the statistical uncertainty of the measurement.

fidence levels. Uncertainties in the predicted values include the uncertainty in the renormalisation and factorisation scales and the combined PDF and α_s uncertainty of the respective PDF set. All PDF predictions are in agreement with the measurement.

For the purpose of determining $f_{LV} \cdot |V_{tb}|$, the measured inclusive cross-sections of the tq and the $\bar{t}q$ process are combined, assuming that each uncertainty is 100 % correlated between the two channels. The statistical uncertainty of the data and the uncertainty due to the limited size of the MC samples, are treated as uncorrelated. The combined cross-section is calculated to be:

$$\begin{aligned}\sigma(tq + \bar{t}q) &= 247 \pm 6\,(\text{stat.}) \pm 45\,(\text{syst.}) \pm 5\,(\text{lumi.})\ \text{pb} \\ &= 247 \pm 46\ \text{pb}.\end{aligned}$$

To estimate the dependence of the measured cross-sections on the assumed top-quark mass, simulated samples with $m_{\text{top}} = 170\,\text{GeV}$ and $m_{\text{top}} = 175\,\text{GeV}$ are used. The measurement is repeated for each top-quark mass. In table 5, the measured cross-sections and their ratio are given.

Single top-quark production in the t-channel proceeds via a Wtb vertex and the measured cross-section is proportional to $(f_{LV} \cdot |V_{tb}|)^2$ as discussed in section 1. The $f_{LV} \cdot |V_{tb}|$ measurement via single top-quark production is independent of assumptions about the number of quark generations or about the unitarity of the CKM matrix. The assumptions made are: $|V_{tb}|$ is much bigger than $|V_{td}|$ and $|V_{ts}|$, which is in agreement with the measurement of $R = \mathcal{B}(t \to Wb)/\sum_{q=d,s,b} \mathcal{B}(t \to Wq)$ [81], the top quark decays exclusively into a W boson and a b-quark, and the Wtb interaction is a left-

m_{top} [GeV]	$\sigma(tq)$ [pb]	$\sigma(\bar{t}q)$ [pb]	$\sigma(tq+\bar{t}q)$ [pb]	R_t
170.0	156 ± 5	93 ± 4	249 ± 6	1.69 ± 0.09
172.5	156 ± 5	91 ± 4	247 ± 6	1.72 ± 0.09
175.0	155 ± 5	92 ± 4	247 ± 6	1.68 ± 0.09

Table 5. Measured values of the cross-sections $\sigma(tq)$, $\sigma(\bar{t}q)$, $\sigma_{\mathrm{tot}}(tq+\bar{t}q)$, and R_t for different simulated top-quark masses. The quoted uncertainties are statistical only.

handed weak coupling like that in the SM. A strategy to relax the first two assumptions and account for production and decay of top quarks via Wts and Wtd vertices is delineated in Ref. [82].

The value of $f_{\mathrm{LV}} \cdot |V_{tb}|$ is extracted by dividing the measured $\sigma(tq+\bar{t}q) = 247 \pm 46$ pb by its value predicted at NLO, $\sigma^{\mathrm{th}}(tq+\bar{t}q) = 217 \pm 10$ pb. Changes in $f_{\mathrm{LV}} \cdot |V_{tb}|$ also affect Wt and $t\bar{b}+\bar{t}b$ production. However, their contributions are small and their variation does not change the t-channel fit result. The result obtained is

$$\begin{aligned} f_{\mathrm{LV}} \cdot |V_{tb}| &= 1.07 \pm 0.01\,(\mathrm{stat.}) \pm 0.09\,(\mathrm{syst.}) \pm 0.02\,(\mathrm{theor.}) \pm 0.01\,(\mathrm{lumi.}) \\ &= 1.07 \pm 0.09. \end{aligned}$$

The experimental uncertainty is 0.09, including the statistical uncertainty, the systematic uncertainties, and the uncertainty in the luminosity. The theoretical uncertainty is 0.02, including scale uncertainties and PDF uncertainties.

Setting $f_{\mathrm{LV}} = 1$ as required by the SM, and assuming a uniform prior of one in $|V_{tb}|^2$ in the interval [0, 1] and a Gaussian-shaped likelihood curve for $|V_{tb}|^2$, a Bayesian lower limit giving $|V_{tb}| > 0.84$ at 95 % CL, is obtained.

10 Conclusion

A measurement of the t-channel single-top-quark and single-top-antiquark production cross-sections is performed in events with a leptonically decaying W boson with 3.2 fb^{-1} of pp collision data at $\sqrt{s} = 13$ TeV recorded with the ATLAS detector at the LHC in 2015. Events are selected by requiring exactly one electron or muon, missing transverse momentum, and two jets with high transverse momentum, exactly one of which is required to be b-tagged.

A binned maximum-likelihood fit to neural-network discriminant distributions yields the following cross-sections:

$$\begin{aligned} \sigma(tq) &= 156 \pm 28 \text{ pb}, \\ \sigma(\bar{t}q) &= 91 \pm 19 \text{ pb}, \\ \sigma(tq+\bar{t}q) &= 247 \pm 46 \text{ pb} \end{aligned}$$

in agreement with SM predictions. The cross-section ratio of tq and $\bar{t}q$ production is found to be $R_t = 1.72 \pm 0.20$. The coupling at the Wtb vertex is determined to be $f_{\mathrm{LV}} \cdot |V_{tb}| = 1.07 \pm 0.09$ and a lower limit on the CKM matrix element is set, giving $|V_{tb}| > 0.84$ at the 95 % CL. These measurements are dominated by systematic uncertainties, from which the uncertainties connected with MC generators are the biggest ones. Further improvements in these generators could lead to smaller expected uncertainties and therefore higher precision in the course of Run 2.

JHEP04(2017)086

Acknowledgments

We thank CERN for the very successful operation of the LHC, as well as the support staff from our institutions without whom ATLAS could not be operated efficiently.

We acknowledge the support of ANPCyT, Argentina; YerPhI, Armenia; ARC, Australia; BMWFW and FWF, Austria; ANAS, Azerbaijan; SSTC, Belarus; CNPq and FAPESP, Brazil; NSERC, NRC and CFI, Canada; CERN; CONICYT, Chile; CAS, MOST and NSFC, China; COLCIENCIAS, Colombia; MSMT CR, MPO CR and VSC CR, Czech Republic; DNRF and DNSRC, Denmark; IN2P3-CNRS, CEA-DSM/IRFU, France; GNSF, Georgia; BMBF, HGF, and MPG, Germany; GSRT, Greece; RGC, Hong Kong SAR, China; ISF, I-CORE and Benoziyo Center, Israel; INFN, Italy; MEXT and JSPS, Japan; CNRST, Morocco; FOM and NWO, Netherlands; RCN, Norway; MNiSW and NCN, Poland; FCT, Portugal; MNE/IFA, Romania; MES of Russia and NRC KI, Russian Federation; JINR; MESTD, Serbia; MSSR, Slovakia; ARRS and MIZŠ, Slovenia; DST/NRF, South Africa; MINECO, Spain; SRC and Wallenberg Foundation, Sweden; SERI, SNSF and Cantons of Bern and Geneva, Switzerland; MOST, Taiwan; TAEK, Turkey; STFC, United Kingdom; DOE and NSF, United States of America. In addition, individual groups and members have received support from BCKDF, the Canada Council, CANARIE, CRC, Compute Canada, FQRNT, and the Ontario Innovation Trust, Canada; EPLANET, ERC, ERDF, FP7, Horizon 2020 and Marie Skłodowska-Curie Actions, European Union; Investissements d'Avenir Labex and Idex, ANR, Région Auvergne and Fondation Partager le Savoir, France; DFG and AvH Foundation, Germany; Herakleitos, Thales and Aristeia programmes co-financed by EU-ESF and the Greek NSRF; BSF, GIF and Minerva, Israel; BRF, Norway; CERCA Programme Generalitat de Catalunya, Generalitat Valenciana, Spain; the Royal Society and Leverhulme Trust, United Kingdom.

The crucial computing support from all WLCG partners is acknowledged gratefully, in particular from CERN, the ATLAS Tier-1 facilities at TRIUMF (Canada), NDGF (Denmark, Norway, Sweden), CC-IN2P3 (France), KIT/GridKA (Germany), INFN-CNAF (Italy), NL-T1 (Netherlands), PIC (Spain), ASGC (Taiwan), RAL (U.K.) and BNL (U.S.A.), the Tier-2 facilities worldwide and large non-WLCG resource providers. Major contributors of computing resources are listed in ref. [83].

References

[1] L. Evans and P. Bryant, *LHC Machine*, 2008 *JINST* **3** S08001 [INSPIRE].

[2] S. Alekhin, J. Blümlein, S. Moch and R. Plačakytė, *Isospin asymmetry of quark distributions and implications for single top-quark production at the LHC*, *Phys. Rev.* **D 94** (2016) 114038 [arXiv:1508.07923] [INSPIRE].

[3] N. Cabibbo, *Unitary Symmetry and Leptonic Decays*, *Phys. Rev. Lett.* **10** (1963) 531 [INSPIRE].

[4] M. Kobayashi and T. Maskawa, *CP Violation in the Renormalizable Theory of Weak Interaction*, *Prog. Theor. Phys.* **49** (1973) 652 [INSPIRE].

- [5] J.A. Aguilar-Saavedra, *A minimal set of top anomalous couplings*, Nucl. Phys. **B 812** (2009) 181 [arXiv:0811.3842] [INSPIRE].
- [6] CMS collaboration, *Measurement of the t-channel single-top-quark production cross section and of the $|V_{tb}|$ CKM matrix element in pp collisions at $\sqrt{s} = 8$ TeV*, JHEP **06** (2014) 090 [arXiv:1403.7366] [INSPIRE].
- [7] J.M. Campbell, R. Frederix, F. Maltoni and F. Tramontano, *Next-to-Leading-Order Predictions for t-Channel Single-Top Production at Hadron Colliders*, Phys. Rev. Lett. **102** (2009) 182003 [arXiv:0903.0005] [INSPIRE].
- [8] P. Kant et al., *HatHor for single top-quark production: Updated predictions and uncertainty estimates for single top-quark production in hadronic collisions*, Comput. Phys. Commun. **191** (2015) 74 [arXiv:1406.4403] [INSPIRE].
- [9] M. Botje et al., *The PDF4LHC Working Group Interim Recommendations*, arXiv:1101.0538 [INSPIRE].
- [10] A.D. Martin, W.J. Stirling, R.S. Thorne and G. Watt, *Parton distributions for the LHC*, Eur. Phys. J. **C 63** (2009) 189 [arXiv:0901.0002] [INSPIRE].
- [11] A.D. Martin, W.J. Stirling, R.S. Thorne and G. Watt, *Uncertainties on α_s in global PDF analyses and implications for predicted hadronic cross sections*, Eur. Phys. J. **C 64** (2009) 653 [arXiv:0905.3531] [INSPIRE].
- [12] H.-L. Lai et al., *New parton distributions for collider physics*, Phys. Rev. **D 82** (2010) 074024 [arXiv:1007.2241] [INSPIRE].
- [13] R.D. Ball et al., *Parton distributions with LHC data*, Nucl. Phys. **B 867** (2013) 244 [arXiv:1207.1303] [INSPIRE].
- [14] N. Kidonakis, *Next-to-next-to-leading-order collinear and soft gluon corrections for t-channel single top quark production*, Phys. Rev. **D 83** (2011) 091503 [arXiv:1103.2792] [INSPIRE].
- [15] N. Kidonakis, *Two-loop soft anomalous dimensions for single top quark associated production with a W^- or H^-*, Phys. Rev. **D 82** (2010) 054018 [arXiv:1005.4451] [INSPIRE].
- [16] N. Kidonakis, *NNLL resummation for s-channel single top quark production*, Phys. Rev. **D 81** (2010) 054028 [arXiv:1001.5034] [INSPIRE].
- [17] M. Brucherseifer, F. Caola and K. Melnikov, *On the NNLO QCD corrections to single-top production at the LHC*, Phys. Lett. **B 736** (2014) 58 [arXiv:1404.7116] [INSPIRE].
- [18] M. Feindt, *A Neural Bayesian Estimator for Conditional Probability Densities*, physics/0402093 [INSPIRE].
- [19] ATLAS collaboration, *Comprehensive measurements of t-channel single top-quark production cross sections at $\sqrt{s} = 7$ TeV with the ATLAS detector*, Phys. Rev. **D 90** (2014) 112006 [arXiv:1406.7844] [INSPIRE].
- [20] ATLAS collaboration, *The ATLAS Experiment at the CERN Large Hadron Collider*, 2008 JINST **3** S08003 [INSPIRE].
- [21] ATLAS collaboration, *ATLAS Insertable B-Layer Technical Design Report*, CERN-LHCC-2010-013 (2010).
- [22] ATLAS collaboration, *2015 start-up trigger menu and initial performance assessment of the ATLAS trigger using Run-2 data*, ATL-DAQ-PUB-2016-001 (2016).

[23] ATLAS collaboration, *The ATLAS Simulation Infrastructure*, *Eur. Phys. J.* **C 70** (2010) 823 [arXiv:1005.4568] [INSPIRE].

[24] GEANT4 collaboration, S. Agostinelli et al., *GEANT4: A simulation toolkit*, *Nucl. Instrum. Meth.* **A 506** (2003) 250 [INSPIRE].

[25] T. Sjöstrand, S. Mrenna and P.Z. Skands, *A Brief Introduction to PYTHIA 8.1*, *Comput. Phys. Commun.* **178** (2008) 852 [arXiv:0710.3820] [INSPIRE].

[26] R. Frederix, E. Re and P. Torrielli, *Single-top t-channel hadroproduction in the four-flavour scheme with POWHEG and aMC@NLO*, *JHEP* **09** (2012) 130 [arXiv:1207.5391] [INSPIRE].

[27] S. Alioli, P. Nason, C. Oleari and E. Re, *A general framework for implementing NLO calculations in shower Monte Carlo programs: the POWHEG BOX*, *JHEP* **06** (2010) 043 [arXiv:1002.2581] [INSPIRE].

[28] T. Sjöstrand, S. Mrenna and P.Z. Skands, *PYTHIA 6.4 Physics and Manual*, *JHEP* **05** (2006) 026 [hep-ph/0603175] [INSPIRE].

[29] P.Z. Skands, *Tuning Monte Carlo Generators: The Perugia Tunes*, *Phys. Rev.* **D 82** (2010) 074018 [arXiv:1005.3457] [INSPIRE].

[30] M. Bahr et al., *HERWIG++ Physics and Manual*, *Eur. Phys. J.* **C 58** (2008) 639 [arXiv:0803.0883] [INSPIRE].

[31] M.H. Seymour and A. Siodmok, *Constraining MPI models using $\sigma_{\rm eff}$ and recent Tevatron and LHC Underlying Event data*, *JHEP* **10** (2013) 113 [arXiv:1307.5015] [INSPIRE].

[32] J. Alwall et al., *The automated computation of tree-level and next-to-leading order differential cross sections and their matching to parton shower simulations*, *JHEP* **07** (2014) 079 [arXiv:1405.0301] [INSPIRE].

[33] E. Re, *Single-top Wt-channel production matched with parton showers using the POWHEG method*, *Eur. Phys. J.* **C 71** (2011) 1547 [arXiv:1009.2450] [INSPIRE].

[34] S. Alioli, P. Nason, C. Oleari and E. Re, *NLO single-top production matched with shower in POWHEG: s- and t-channel contributions*, *JHEP* **09** (2009) 111 [*Erratum ibid.* **02** (2010) 011] [arXiv:0907.4076] [INSPIRE].

[35] S. Frixione, P. Nason and G. Ridolfi, *A positive-weight next-to-leading-order Monte Carlo for heavy flavour hadroproduction*, *JHEP* **09** (2007) 126 [arXiv:0707.3088] [INSPIRE].

[36] D.J. Lange, *The EvtGen particle decay simulation package*, *Nucl. Instrum. Meth.* **A 462** (2001) 152 [INSPIRE].

[37] T. Gleisberg et al., *Event generation with SHERPA 1.1*, *JHEP* **02** (2009) 007 [arXiv:0811.4622] [INSPIRE].

[38] T. Gleisberg and S. Hoeche, *Comix, a new matrix element generator*, *JHEP* **12** (2008) 039 [arXiv:0808.3674] [INSPIRE].

[39] F. Cascioli, P. Maierhofer and S. Pozzorini, *Scattering Amplitudes with Open Loops*, *Phys. Rev. Lett.* **108** (2012) 111601 [arXiv:1111.5206] [INSPIRE].

[40] S. Schumann and F. Krauss, *A parton shower algorithm based on Catani-Seymour dipole factorisation*, *JHEP* **03** (2008) 038 [arXiv:0709.1027] [INSPIRE].

[41] S. Hoeche, F. Krauss, M. Schonherr and F. Siegert, *QCD matrix elements + parton showers: The NLO case*, *JHEP* **04** (2013) 027 [arXiv:1207.5030] [INSPIRE].

[42] NNPDF collaboration, R.D. Ball et al., *Parton distributions for the LHC Run II*, JHEP **04** (2015) 040 [arXiv:1410.8849] [INSPIRE].

[43] ATLAS collaboration, *Estimation of non-prompt and fake lepton backgrounds in final states with top quarks produced in proton-proton collisions at $\sqrt{s} = 8$ TeV with the ATLAS detector*, ATLAS-CONF-2014-058 (2014).

[44] ATLAS collaboration, *Electron reconstruction and identification efficiency measurements with the ATLAS detector using the 2011 LHC proton-proton collision data*, Eur. Phys. J. **C 74** (2014) 2941 [arXiv:1404.2240] [INSPIRE].

[45] ATLAS collaboration, *Electron efficiency measurements with the ATLAS detector using the 2012 LHC proton-proton collision data*, ATLAS-CONF-2014-032 (2014).

[46] ATLAS collaboration, *Measurement of the $t\bar{t}$ production cross-section using $e\mu$ events with b-tagged jets in pp collisions at $\sqrt{s} = 13$ TeV with the ATLAS detector*, Phys. Lett. **B 761** (2016) 136 [arXiv:1606.02699] [INSPIRE].

[47] M. Cacciari, G.P. Salam and G. Soyez, *The anti-k_T jet clustering algorithm*, JHEP **04** (2008) 063 [arXiv:0802.1189] [INSPIRE].

[48] ATLAS collaboration, *Monte Carlo Calibration and Combination of In-situ Measurements of Jet Energy Scale, Jet Energy Resolution and Jet Mass in ATLAS*, ATLAS-CONF-2015-037 (2015).

[49] ATLAS collaboration, *Performance of pile-up mitigation techniques for jets in pp collisions at $\sqrt{s} = 8$ TeV using the ATLAS detector*, Eur. Phys. J. **C 76** (2016) 581 [arXiv:1510.03823] [INSPIRE].

[50] ATLAS collaboration, *Calibration of the performance of b-tagging for c and light-flavour jets in the 2012 ATLAS data*, ATLAS-CONF-2014-046 (2014).

[51] ATLAS collaboration, *Calibration of b-tagging using dileptonic top pair events in a combinatorial likelihood approach with the ATLAS experiment*, ATLAS-CONF-2014-004 (2014).

[52] ATLAS collaboration, *Performance of the ATLAS muon trigger in pp collisions at $\sqrt{s} = 8$ TeV*, Eur. Phys. J. **C 75** (2015) 120 [arXiv:1408.3179] [INSPIRE].

[53] M. Cacciari, M. Czakon, M. Mangano, A. Mitov and P. Nason, *Top-pair production at hadron colliders with next-to-next-to-leading logarithmic soft-gluon resummation*, Phys. Lett. **B 710** (2012) 612 [arXiv:1111.5869] [INSPIRE].

[54] P. Bärnreuther, M. Czakon and A. Mitov, *Percent Level Precision Physics at the Tevatron: First Genuine NNLO QCD Corrections to $q\bar{q} \to t\bar{t} + X$*, Phys. Rev. Lett. **109** (2012) 132001 [arXiv:1204.5201] [INSPIRE].

[55] M. Czakon and A. Mitov, *NNLO corrections to top-pair production at hadron colliders: the all-fermionic scattering channels*, JHEP **12** (2012) 054 [arXiv:1207.0236] [INSPIRE].

[56] M. Czakon and A. Mitov, *NNLO corrections to top pair production at hadron colliders: the quark-gluon reaction*, JHEP **01** (2013) 080 [arXiv:1210.6832] [INSPIRE].

[57] M. Czakon, P. Fiedler and A. Mitov, *Total Top-Quark Pair-Production Cross section at Hadron Colliders Through $O(\alpha_S^4)$*, Phys. Rev. Lett. **110** (2013) 252004 [arXiv:1303.6254] [INSPIRE].

[58] M. Czakon and A. Mitov, *Top++: A Program for the Calculation of the Top-Pair Cross-Section at Hadron Colliders*, Comput. Phys. Commun. **185** (2014) 2930 [arXiv:1112.5675] [INSPIRE].

[59] C. Anastasiou, L.J. Dixon, K. Melnikov and F. Petriello, *High precision QCD at hadron colliders: Electroweak gauge boson rapidity distributions at NNLO*, Phys. Rev. **D 69** (2004) 094008 [hep-ph/0312266] [INSPIRE].

[60] M. Feindt and U. Kerzel, *The NeuroBayes neural network package*, Nucl. Instrum. Meth. **A 559** (2006) 190 [INSPIRE].

[61] ATLAS collaboration, *Electron and photon energy calibration with the ATLAS detector using LHC Run 1 data*, Eur. Phys. J. **C 74** (2014) 3071 [arXiv:1407.5063] [INSPIRE].

[62] ATLAS collaboration, *Electron identification measurements in ATLAS using* $\sqrt{s} = 13$ *TeV data with 50 ns bunch spacing*, ATL-PHYS-PUB-2015-041 (2015).

[63] ATLAS collaboration, *Muon reconstruction performance of the ATLAS detector in proton-proton collision data at* $\sqrt{s} = 13$ *TeV*, Eur. Phys. J. **C 76** (2016) 292 [arXiv:1603.05598] [INSPIRE].

[64] ATLAS collaboration, *Jet energy measurement and its systematic uncertainty in proton-proton collisions at* $\sqrt{s} = 7$ *TeV with the ATLAS detector*, Eur. Phys. J. **C 75** (2015) 17 [arXiv:1406.0076] [INSPIRE].

[65] ATLAS collaboration, *Jet Calibration and Systematic Uncertainties for Jets Reconstructed in the ATLAS Detector at* $\sqrt{s} = 13$ *TeV*, ATL-PHYS-PUB-2015-015 (2015).

[66] ATLAS collaboration, *Jet energy resolution in proton-proton collisions at* $\sqrt{s} = 7$ *TeV recorded in 2010 with the ATLAS detector*, Eur. Phys. J. **C 73** (2013) 2306 [arXiv:1210.6210] [INSPIRE].

[67] ATLAS collaboration, *Comparison of Monte Carlo generator predictions to ATLAS measurements of top pair production at 7 TeV*, ATL-PHYS-PUB-2015-002 (2015).

[68] J. Butterworth et al., *PDF4LHC recommendations for LHC Run II*, J. Phys. **G 43** (2016) 023001 [arXiv:1510.03865] [INSPIRE].

[69] ATLAS collaboration, *Measurements of the W production cross sections in association with jets with the ATLAS detector*, Eur. Phys. J. **C 75** (2015) 82 [arXiv:1409.8639] [INSPIRE].

[70] ATLAS collaboration, *Measurement of the Inclusive and Fiducial Cross-Section of Single Top-Quark t-Channel Events in pp Collisions at* $\sqrt{s} = 8$ *TeV*, ATLAS-CONF-2014-007 (2014).

[71] ATLAS collaboration, *Improved luminosity determination in pp collisions at* $\sqrt{s} = 7$ *TeV using the ATLAS detector at the LHC*, Eur. Phys. J. **C 73** (2013) 2518 [arXiv:1302.4393] [INSPIRE].

[72] ATLAS collaboration, *Luminosity determination in pp collisions at* $\sqrt{s} = 8$ *TeV using the ATLAS detector at the LHC*, to be submitted to *Eur. Phys. J. C* (2016).

[73] S. Dulat et al., *New parton distribution functions from a global analysis of quantum chromodynamics*, Phys. Rev. **D 93** (2016) 033006 [arXiv:1506.07443] [INSPIRE].

[74] L.A. Harland-Lang, A.D. Martin, P. Motylinski and R.S. Thorne, *Parton distributions in the LHC era: MMHT 2014 PDFs*, Eur. Phys. J. **C 75** (2015) 204 [arXiv:1412.3989] [INSPIRE].

[75] R.D. Ball et al., *Impact of Heavy Quark Masses on Parton Distributions and LHC Phenomenology*, Nucl. Phys. **B 849** (2011) 296 [arXiv:1101.1300] [INSPIRE].

[76] P. Jimenez-Delgado and E. Reya, *Delineating parton distributions and the strong coupling*, Phys. Rev. **D 89** (2014) 074049 [arXiv:1403.1852] [INSPIRE].

[77] S. Alekhin, J. Blumlein and S. Moch, *Parton Distribution Functions and Benchmark Cross sections at NNLO*, Phys. Rev. **D 86** (2012) 054009 [arXiv:1202.2281] [INSPIRE].

[78] ZEUS, H1 collaborations, F.D. Aaron et al., *Combined Measurement and QCD Analysis of the Inclusive* $e^{\pm}p$ *Scattering Cross sections at HERA*, JHEP **01** (2010) 109 [arXiv:0911.0884] [INSPIRE].

[79] ZEUS, H1 collaborations, H. Abramowicz et al., *Combination of measurements of inclusive deep inelastic $e^{\pm}p$ scattering cross sections and QCD analysis of HERA data*, Eur. Phys. J. **C 75** (2015) 580 [arXiv:1506.06042] [INSPIRE].

[80] ATLAS collaboration, *Determination of the strange quark density of the proton from ATLAS measurements of the $W \to \ell\nu$ and $Z \to \ell\ell$ cross sections*, Phys. Rev. Lett. **109** (2012) 012001 [arXiv:1203.4051] [INSPIRE].

[81] CMS collaboration, *Measurement of the ratio $\mathcal{B}(t \to Wb)/\mathcal{B}(t \to Wq)$ in pp collisions at $\sqrt{s} = 8$ TeV*, Phys. Lett. **B 736** (2014) 33 [arXiv:1404.2292] [INSPIRE].

[82] H. Lacker et al., *Model-independent extraction of $|V_{tq}|$ matrix elements from top-quark measurements at hadron colliders*, Eur. Phys. J. **C 72** (2012) 2048 [arXiv:1202.4694] [INSPIRE].

[83] ATLAS collaboration, *ATLAS Computing Acknowledgements 2016-2017*, ATL-GEN-PUB-2016-002 (2016).

The ATLAS collaboration

M. Aaboud[136d], G. Aad[87], B. Abbott[114], J. Abdallah[8], O. Abdinov[12], B. Abeloos[118], R. Aben[108], O.S. AbouZeid[138], N.L. Abraham[152], H. Abramowicz[156], H. Abreu[155], R. Abreu[117], Y. Abulaiti[149a,149b], B.S. Acharya[168a,168b,a], S. Adachi[158], L. Adamczyk[40a], D.L. Adams[27], J. Adelman[109], S. Adomeit[101], T. Adye[132], A.A. Affolder[76], T. Agatonovic-Jovin[14], J.A. Aguilar-Saavedra[127a,127f], S.P. Ahlen[24], F. Ahmadov[67,b], G. Aielli[134a,134b], H. Akerstedt[149a,149b], T.P.A. Åkesson[83], A.V. Akimov[97], G.L. Alberghi[22a,22b], J. Albert[173], S. Albrand[57], M.J. Alconada Verzini[73], M. Aleksa[32], I.N. Aleksandrov[67], C. Alexa[28b], G. Alexander[156], T. Alexopoulos[10], M. Alhroob[114], B. Ali[129], M. Aliev[75a,75b], G. Alimonti[93a], J. Alison[33], S.P. Alkire[37], B.M.M. Allbrooke[152], B.W. Allen[117], P.P. Allport[19], A. Aloisio[105a,105b], A. Alonso[38], F. Alonso[73], C. Alpigiani[139], A.A. Alshehri[55], M. Alstaty[87], B. Alvarez Gonzalez[32], D. Álvarez Piqueras[171], M.G. Alviggi[105a,105b], B.T. Amadio[16], K. Amako[68], Y. Amaral Coutinho[26a], C. Amelung[25], D. Amidei[91], S.P. Amor Dos Santos[127a,127c], A. Amorim[127a,127b], S. Amoroso[32], G. Amundsen[25], C. Anastopoulos[142], L.S. Ancu[51], N. Andari[19], T. Andeen[11], C.F. Anders[60b], G. Anders[32], J.K. Anders[76], K.J. Anderson[33], A. Andreazza[93a,93b], V. Andrei[60a], S. Angelidakis[9], I. Angelozzi[108], A. Angerami[37], F. Anghinolfi[32], A.V. Anisenkov[110,c], N. Anjos[13], A. Annovi[125a,125b], C. Antel[60a], M. Antonelli[49], A. Antonov[99,*], F. Anulli[133a], M. Aoki[68], L. Aperio Bella[19], G. Arabidze[92], Y. Arai[68], J.P. Araque[127a], A.T.H. Arce[47], F.A. Arduh[73], J-F. Arguin[96], S. Argyropoulos[65], M. Arik[20a], A.J. Armbruster[146], L.J. Armitage[78], O. Arnaez[32], H. Arnold[50], M. Arratia[30], O. Arslan[23], A. Artamonov[98], G. Artoni[121], S. Artz[85], S. Asai[158], N. Asbah[44], A. Ashkenazi[156], B. Åsman[149a,149b], L. Asquith[152], K. Assamagan[27], R. Astalos[147a], M. Atkinson[170], N.B. Atlay[144], K. Augsten[129], G. Avolio[32], B. Axen[16], M.K. Ayoub[118], G. Azuelos[96,d], M.A. Baak[32], A.E. Baas[60a], M.J. Baca[19], H. Bachacou[137], K. Bachas[75a,75b], M. Backes[121], M. Backhaus[32], P. Bagiacchi[133a,133b], P. Bagnaia[133a,133b], Y. Bai[35a], J.T. Baines[132], O.K. Baker[180], E.M. Baldin[110,c], P. Balek[176], T. Balestri[151], F. Balli[137], W.K. Balunas[123], E. Banas[41], Sw. Banerjee[177,e], A.A.E. Bannoura[179], L. Barak[32], E.L. Barberio[90], D. Barberis[52a,52b], M. Barbero[87], T. Barillari[102], M-S Barisits[32], T. Barklow[146], N. Barlow[30], S.L. Barnes[86], B.M. Barnett[132], R.M. Barnett[16], Z. Barnovska-Blenessy[5], A. Baroncelli[135a], G. Barone[25], A.J. Barr[121], L. Barranco Navarro[171], F. Barreiro[84], J. Barreiro Guimarães da Costa[35a], R. Bartoldus[146], A.E. Barton[74], P. Bartos[147a], A. Basalaev[124], A. Bassalat[118,f], R.L. Bates[55], S.J. Batista[162], J.R. Batley[30], M. Battaglia[138], M. Bauce[133a,133b], F. Bauer[137], H.S. Bawa[146,g], J.B. Beacham[112], M.D. Beattie[74], T. Beau[82], P.H. Beauchemin[166], P. Bechtle[23], H.P. Beck[18,h], K. Becker[121], M. Becker[85], M. Beckingham[174], C. Becot[111], A.J. Beddall[20e], A. Beddall[20b], V.A. Bednyakov[67], M. Bedognetti[108], C.P. Bee[151], L.J. Beemster[108], T.A. Beermann[32], M. Begel[27], J.K. Behr[44], C. Belanger-Champagne[89], A.S. Bell[80], G. Bella[156], L. Bellagamba[22a], A. Bellerive[31], M. Bellomo[88], K. Belotskiy[99], O. Beltramello[32], N.L. Belyaev[99], O. Benary[156,*], D. Benchekroun[136a], M. Bender[101], K. Bendtz[149a,149b], N. Benekos[10], Y. Benhammou[156], E. Benhar Noccioli[180], J. Benitez[65], D.P. Benjamin[47], J.R. Bensinger[25], S. Bentvelsen[108], L. Beresford[121], M. Beretta[49], D. Berge[108], E. Bergeaas Kuutmann[169], N. Berger[5], J. Beringer[16], S. Berlendis[57], N.R. Bernard[88], C. Bernius[111], F.U. Bernlochner[23], T. Berry[79], P. Berta[130], C. Bertella[85], G. Bertoli[149a,149b], F. Bertolucci[125a,125b], I.A. Bertram[74], C. Bertsche[44], D. Bertsche[114], G.J. Besjes[38], O. Bessidskaia Bylund[149a,149b], M. Bessner[44], N. Besson[137], C. Betancourt[50], A. Bethani[57], S. Bethke[102], A.J. Bevan[78], R.M. Bianchi[126], L. Bianchini[25], M. Bianco[32], O. Biebel[101], D. Biedermann[17], R. Bielski[86], N.V. Biesuz[125a,125b], M. Biglietti[135a], J. Bilbao De Mendizabal[51], T.R.V. Billoud[96], H. Bilokon[49], M. Bindi[56], S. Binet[118], A. Bingul[20b], C. Bini[133a,133b], S. Biondi[22a,22b], T. Bisanz[56], D.M. Bjergaard[47], C.W. Black[153], J.E. Black[146], K.M. Black[24], D. Blackburn[139], R.E. Blair[6], J.-B. Blanchard[137], T. Blazek[147a], I. Bloch[44], C. Blocker[25], A. Blue[55], W. Blum[85,*], U. Blumenschein[56], S. Blunier[34a], G.J. Bobbink[108], V.S. Bobrovnikov[110,c], S.S. Bocchetta[83], A. Bocci[47], C. Bock[101], M. Boehler[50], D. Boerner[179], J.A. Bogaerts[32], D. Bogavac[14], A.G. Bogdanchikov[110], C. Bohm[149a],

V. Boisvert[79], P. Bokan[14], T. Bold[40a], A.S. Boldyrev[168a,168c], M. Bomben[82], M. Bona[78], M. Boonekamp[137], A. Borisov[131], G. Borissov[74], J. Bortfeldt[32], D. Bortoletto[121], V. Bortolotto[62a,62b,62c], K. Bos[108], D. Boscherini[22a], M. Bosman[13], J.D. Bossio Sola[29], J. Boudreau[126], J. Bouffard[2], E.V. Bouhova-Thacker[74], D. Boumediene[36], C. Bourdarios[118], S.K. Boutle[55], A. Boveia[32], J. Boyd[32], I.R. Boyko[67], J. Bracinik[19], A. Brandt[8], G. Brandt[56], O. Brandt[60a], U. Bratzler[159], B. Brau[88], J.E. Brau[117], W.D. Breaden Madden[55], K. Brendlinger[123], A.J. Brennan[90], L. Brenner[108], R. Brenner[169], S. Bressler[176], T.M. Bristow[48], D. Britton[55], D. Britzger[44], F.M. Brochu[30], I. Brock[23], R. Brock[92], G. Brooijmans[37], T. Brooks[79], W.K. Brooks[34b], J. Brosamer[16], E. Brost[109], J.H Broughton[19], P.A. Bruckman de Renstrom[41], D. Bruncko[147b], R. Bruneliere[50], A. Bruni[22a], G. Bruni[22a], L.S. Bruni[108], BH Brunt[30], M. Bruschi[22a], N. Bruscino[23], P. Bryant[33], L. Bryngemark[83], T. Buanes[15], Q. Buat[145], P. Buchholz[144], A.G. Buckley[55], I.A. Budagov[67], F. Buehrer[50], M.K. Bugge[120], O. Bulekov[99], D. Bullock[8], H. Burckhart[32], S. Burdin[76], C.D. Burgard[50], B. Burghgrave[109], K. Burka[41], S. Burke[132], I. Burmeister[45], J.T.P. Burr[121], E. Busato[36], D. Büscher[50], V. Büscher[85], P. Bussey[55], J.M. Butler[24], C.M. Buttar[55], J.M. Butterworth[80], P. Butti[108], W. Buttinger[27], A. Buzatu[55], A.R. Buzykaev[110,c], S. Cabrera Urbán[171], D. Caforio[129], V.M. Cairo[39a,39b], O. Cakir[4a], N. Calace[51], P. Calafiura[16], A. Calandri[87], G. Calderini[82], P. Calfayan[101], G. Callea[39a,39b], L.P. Caloba[26a], S. Calvente Lopez[84], D. Calvet[36], S. Calvet[36], T.P. Calvet[87], R. Camacho Toro[33], S. Camarda[32], P. Camarri[134a,134b], D. Cameron[120], R. Caminal Armadans[170], C. Camincher[57], S. Campana[32], M. Campanelli[80], A. Camplani[93a,93b], A. Campoverde[144], V. Canale[105a,105b], A. Canepa[164a], M. Cano Bret[141], J. Cantero[115], T. Cao[42], M.D.M. Capeans Garrido[32], I. Caprini[28b], M. Caprini[28b], M. Capua[39a,39b], R.M. Carbone[37], R. Cardarelli[134a], F. Cardillo[50], I. Carli[130], T. Carli[32], G. Carlino[105a], L. Carminati[93a,93b], S. Caron[107], E. Carquin[34b], G.D. Carrillo-Montoya[32], J.R. Carter[30], J. Carvalho[127a,127c], D. Casadei[19], M.P. Casado[13,i], M. Casolino[13], D.W. Casper[167], E. Castaneda-Miranda[148a], R. Castelijn[108], A. Castelli[108], V. Castillo Gimenez[171], N.F. Castro[127a,j], A. Catinaccio[32], J.R. Catmore[120], A. Cattai[32], J. Caudron[23], V. Cavaliere[170], E. Cavallaro[13], D. Cavalli[93a], M. Cavalli-Sforza[13], V. Cavasinni[125a,125b], F. Ceradini[135a,135b], L. Cerda Alberich[171], A.S. Cerqueira[26b], A. Cerri[152], L. Cerrito[134a,134b], F. Cerutti[16], M. Cerv[32], A. Cervelli[18], S.A. Cetin[20d], A. Chafaq[136a], D. Chakraborty[109], S.K. Chan[58], Y.L. Chan[62a], P. Chang[170], J.D. Chapman[30], D.G. Charlton[19], A. Chatterjee[51], C.C. Chau[162], C.A. Chavez Barajas[152], S. Che[112], S. Cheatham[168a,168c], A. Chegwidden[92], S. Chekanov[6], S.V. Chekulaev[164a], G.A. Chelkov[67,k], M.A. Chelstowska[91], C. Chen[66], H. Chen[27], K. Chen[151], S. Chen[35b], S. Chen[158], X. Chen[35c], Y. Chen[69], H.C. Cheng[91], H.J Cheng[35a], Y. Cheng[33], A. Cheplakov[67], E. Cheremushkina[131], R. Cherkaoui El Moursli[136e], V. Chernyatin[27,*], E. Cheu[7], L. Chevalier[137], V. Chiarella[49], G. Chiarelli[125a,125b], G. Chiodini[75a], A.S. Chisholm[32], A. Chitan[28b], M.V. Chizhov[67], K. Choi[63], A.R. Chomont[36], S. Chouridou[9], B.K.B. Chow[101], V. Christodoulou[80], D. Chromek-Burckhart[32], J. Chudoba[128], A.J. Chuinard[89], J.J. Chwastowski[41], L. Chytka[116], G. Ciapetti[133a,133b], A.K. Ciftci[4a], D. Cinca[45], V. Cindro[77], I.A. Cioara[23], C. Ciocca[22a,22b], A. Ciocio[16], F. Cirotto[105a,105b], Z.H. Citron[176], M. Citterio[93a], M. Ciubancan[28b], A. Clark[51], B.L. Clark[58], M.R. Clark[37], P.J. Clark[48], R.N. Clarke[16], C. Clement[149a,149b], Y. Coadou[87], M. Cobal[168a,168c], A. Coccaro[51], J. Cochran[66], L. Colasurdo[107], B. Cole[37], A.P. Colijn[108], J. Collot[57], T. Colombo[167], G. Compostella[102], P. Conde Muiño[127a,127b], E. Coniavitis[50], S.H. Connell[148b], I.A. Connelly[79], V. Consorti[50], S. Constantinescu[28b], G. Conti[32], F. Conventi[105a,l], M. Cooke[16], B.D. Cooper[80], A.M. Cooper-Sarkar[121], K.J.R. Cormier[162], T. Cornelissen[179], M. Corradi[133a,133b], F. Corriveau[89,m], A. Cortes-Gonzalez[32], G. Cortiana[102], G. Costa[93a], M.J. Costa[171], D. Costanzo[142], G. Cottin[30], G. Cowan[79], B.E. Cox[86], K. Cranmer[111], S.J. Crawley[55], G. Cree[31], S. Crépé-Renaudin[57], F. Crescioli[82], W.A. Cribbs[149a,149b], M. Crispin Ortuzar[121], M. Cristinziani[23], V. Croft[107], G. Crosetti[39a,39b], A. Cueto[84], T. Cuhadar Donszelmann[142], J. Cummings[180], M. Curatolo[49], J. Cúth[85], H. Czirr[144], P. Czodrowski[3], G. D'amen[22a,22b], S. D'Auria[55], M. D'Onofrio[76], M.J. Da Cunha Sargedas De Sousa[127a,127b], C. Da Via[86], W. Dabrowski[40a], T. Dado[147a], T. Dai[91], O. Dale[15], F. Dallaire[96], C. Dallapiccola[88], M. Dam[38], J.R. Dandoy[33], N.P. Dang[50], A.C. Daniells[19], N.S. Dann[86], M. Danninger[172],

M. Dano Hoffmann[137], V. Dao[50], G. Darbo[52a], S. Darmora[8], J. Dassoulas[3], A. Dattagupta[117], W. Davey[23], C. David[173], T. Davidek[130], M. Davies[156], P. Davison[80], E. Dawe[90], I. Dawson[142], K. De[8], R. de Asmundis[105a], A. De Benedetti[114], S. De Castro[22a,22b], S. De Cecco[82], N. De Groot[107], P. de Jong[108], H. De la Torre[92], F. De Lorenzi[66], A. De Maria[56], D. De Pedis[133a], A. De Salvo[133a], U. De Sanctis[152], A. De Santo[152], J.B. De Vivie De Regie[118], W.J. Dearnaley[74], R. Debbe[27], C. Debenedetti[138], D.V. Dedovich[67], N. Dehghanian[3], I. Deigaard[108], M. Del Gaudio[39a,39b], J. Del Peso[84], T. Del Prete[125a,125b], D. Delgove[118], F. Deliot[137], C.M. Delitzsch[51], A. Dell'Acqua[32], L. Dell'Asta[24], M. Dell'Orso[125a,125b], M. Della Pietra[105a,l], D. della Volpe[51], M. Delmastro[5], P.A. Delsart[57], D.A. DeMarco[162], S. Demers[180], M. Demichev[67], A. Demilly[82], S.P. Denisov[131], D. Denysiuk[137], D. Derendarz[41], J.E. Derkaoui[136d], F. Derue[82], P. Dervan[76], K. Desch[23], C. Deterre[44], K. Dette[45], P.O. Deviveiros[32], A. Dewhurst[132], S. Dhaliwal[25], A. Di Ciaccio[134a,134b], L. Di Ciaccio[5], W.K. Di Clemente[123], C. Di Donato[133a,133b], A. Di Girolamo[32], B. Di Girolamo[32], B. Di Micco[135a,135b], R. Di Nardo[32], A. Di Simone[50], R. Di Sipio[162], D. Di Valentino[31], C. Diaconu[87], M. Diamond[162], F.A. Dias[48], M.A. Diaz[34a], E.B. Diehl[91], J. Dietrich[17], S. Díez Cornell[44], A. Dimitrievska[14], J. Dingfelder[23], P. Dita[28b], S. Dita[28b], F. Dittus[32], F. Djama[87], T. Djobava[53b], J.I. Djuvsland[60a], M.A.B. do Vale[26c], D. Dobos[32], M. Dobre[28b], C. Doglioni[83], J. Dolejsi[130], Z. Dolezal[130], M. Donadelli[26d], S. Donati[125a,125b], P. Dondero[122a,122b], J. Donini[36], J. Dopke[132], A. Doria[105a], M.T. Dova[73], A.T. Doyle[55], E. Drechsler[56], M. Dris[10], Y. Du[140], J. Duarte-Campderros[156], E. Duchovni[176], G. Duckeck[101], O.A. Ducu[96,n], D. Duda[108], A. Dudarev[32], A.Chr. Dudder[85], E.M. Duffield[16], L. Duflot[118], M. Dührssen[32], M. Dumancic[176], M. Dunford[60a], H. Duran Yildiz[4a], M. Düren[54], A. Durglishvili[53b], D. Duschinger[46], B. Dutta[44], M. Dyndal[44], C. Eckardt[44], K.M. Ecker[102], R.C. Edgar[91], N.C. Edwards[48], T. Eifert[32], G. Eigen[15], K. Einsweiler[16], T. Ekelof[169], M. El Kacimi[136c], V. Ellajosyula[87], M. Ellert[169], S. Elles[5], F. Ellinghaus[179], A.A. Elliot[173], N. Ellis[32], J. Elmsheuser[27], M. Elsing[32], D. Emeliyanov[132], Y. Enari[158], O.C. Endner[85], J.S. Ennis[174], J. Erdmann[45], A. Ereditato[18], G. Ernis[179], J. Ernst[2], M. Ernst[27], S. Errede[170], E. Ertel[85], M. Escalier[118], H. Esch[45], C. Escobar[126], B. Esposito[49], A.I. Etienvre[137], E. Etzion[156], H. Evans[63], A. Ezhilov[124], M. Ezzi[136e], F. Fabbri[22a,22b], L. Fabbri[22a,22b], G. Facini[33], R.M. Fakhrutdinov[131], S. Falciano[133a], R.J. Falla[80], J. Faltova[32], Y. Fang[35a], M. Fanti[93a,93b], A. Farbin[8], A. Farilla[135a], C. Farina[126], E.M. Farina[122a,122b], T. Farooque[13], S. Farrell[16], S.M. Farrington[174], P. Farthouat[32], F. Fassi[136e], P. Fassnacht[32], D. Fassouliotis[9], M. Faucci Giannelli[79], A. Favareto[52a,52b], W.J. Fawcett[121], L. Fayard[118], O.L. Fedin[124,o], W. Fedorko[172], S. Feigl[120], L. Feligioni[87], C. Feng[140], E.J. Feng[32], H. Feng[91], A.B. Fenyuk[131], L. Feremenga[8], P. Fernandez Martinez[171], S. Fernandez Perez[13], J. Ferrando[44], A. Ferrari[169], P. Ferrari[108], R. Ferrari[122a], D.E. Ferreira de Lima[60b], A. Ferrer[171], D. Ferrere[51], C. Ferretti[91], A. Ferretto Parodi[52a,52b], F. Fiedler[85], A. Filipčič[77], M. Filipuzzi[44], F. Filthaut[107], M. Fincke-Keeler[173], K.D. Finelli[153], M.C.N. Fiolhais[127a,127c], L. Fiorini[171], A. Firan[42], A. Fischer[2], C. Fischer[13], J. Fischer[179], W.C. Fisher[92], N. Flaschel[44], I. Fleck[144], P. Fleischmann[91], G.T. Fletcher[142], R.R.M. Fletcher[123], T. Flick[179], L.R. Flores Castillo[62a], M.J. Flowerdew[102], G.T. Forcolin[86], A. Formica[137], A. Forti[86], A.G. Foster[19], D. Fournier[118], H. Fox[74], S. Fracchia[13], P. Francavilla[82], M. Franchini[22a,22b], D. Francis[32], L. Franconi[120], M. Franklin[58], M. Frate[167], M. Fraternali[122a,122b], D. Freeborn[80], S.M. Fressard-Batraneanu[32], F. Friedrich[46], D. Froidevaux[32], J.A. Frost[121], C. Fukunaga[159], E. Fullana Torregrosa[85], T. Fusayasu[103], J. Fuster[171], C. Gabaldon[57], O. Gabizon[179], A. Gabrielli[22a,22b], A. Gabrielli[16], G.P. Gach[40a], S. Gadatsch[32], S. Gadomski[79], G. Gagliardi[52a,52b], L.G. Gagnon[96], P. Gagnon[63], C. Galea[107], B. Galhardo[127a,127c], E.J. Gallas[121], B.J. Gallop[132], P. Gallus[129], G. Galster[38], K.K. Gan[112], J. Gao[59], Y. Gao[48], Y.S. Gao[146,g], F.M. Garay Walls[48], C. García[171], J.E. García Navarro[171], M. Garcia-Sciveres[16], R.W. Gardner[33], N. Garelli[146], V. Garonne[120], A. Gascon Bravo[44], K. Gasnikova[44], C. Gatti[49], A. Gaudiello[52a,52b], G. Gaudio[122a], L. Gauthier[96], I.L. Gavrilenko[97], C. Gay[172], G. Gaycken[23], E.N. Gazis[10], Z. Gecse[172], C.N.P. Gee[132], Ch. Geich-Gimbel[23], M. Geisen[85], M.P. Geisler[60a], K. Gellerstedt[149a,149b], C. Gemme[52a], M.H. Genest[57], C. Geng[59,p], S. Gentile[133a,133b], C. Gentsos[157],

JHEP04(2017)086

S. George[79], D. Gerbaudo[13], A. Gershon[156], S. Ghasemi[144], M. Ghneimat[23], B. Giacobbe[22a], S. Giagu[133a,133b], P. Giannetti[125a,125b], B. Gibbard[27], S.M. Gibson[79], M. Gignac[172], M. Gilchriese[16], T.P.S. Gillam[30], D. Gillberg[31], G. Gilles[179], D.M. Gingrich[3,d], N. Giokaris[9], M.P. Giordani[168a,168c], F.M. Giorgi[22a], F.M. Giorgi[17], P.F. Giraud[137], P. Giromini[58], D. Giugni[93a], F. Giuli[121], C. Giuliani[102], M. Giulini[60b], B.K. Gjelsten[120], S. Gkaitatzis[157], I. Gkialas[157], E.L. Gkougkousis[118], L.K. Gladilin[100], C. Glasman[84], J. Glatzer[50], P.C.F. Glaysher[48], A. Glazov[44], M. Goblirsch-Kolb[25], J. Godlewski[41], S. Goldfarb[90], T. Golling[51], D. Golubkov[131], A. Gomes[127a,127b,127d], R. Gonçalo[127a], J. Goncalves Pinto Firmino Da Costa[137], G. Gonella[50], L. Gonella[19], A. Gongadze[67], S. González de la Hoz[171], S. Gonzalez-Sevilla[51], L. Goossens[32], P.A. Gorbounov[98], H.A. Gordon[27], I. Gorelov[106], B. Gorini[32], E. Gorini[75a,75b], A. Gorišek[77], E. Gornicki[41], A.T. Goshaw[47], C. Gössling[45], M.I. Gostkin[67], C.R. Goudet[118], D. Goujdami[136c], A.G. Goussiou[139], N. Govender[148b,q], E. Gozani[155], L. Graber[56], I. Grabowska-Bold[40a], P.O.J. Gradin[57], P. Grafström[22a,22b], J. Gramling[51], E. Gramstad[120], S. Grancagnolo[17], V. Gratchev[124], P.M. Gravila[28e], H.M. Gray[32], E. Graziani[135a], Z.D. Greenwood[81,r], C. Grefe[23], K. Gregersen[80], I.M. Gregor[44], P. Grenier[146], K. Grevtsov[5], J. Griffiths[8], A.A. Grillo[138], K. Grimm[74], S. Grinstein[13,s], Ph. Gris[36], J.-F. Grivaz[118], S. Groh[85], E. Gross[176], J. Grosse-Knetter[56], G.C. Grossi[81], Z.J. Grout[80], L. Guan[91], W. Guan[177], J. Guenther[64], F. Guescini[51], D. Guest[167], O. Gueta[156], E. Guido[52a,52b], T. Guillemin[5], S. Guindon[2], U. Gul[55], C. Gumpert[32], J. Guo[141], Y. Guo[59,p], R. Gupta[42], S. Gupta[121], G. Gustavino[133a,133b], P. Gutierrez[114], N.G. Gutierrez Ortiz[80], C. Gutschow[46], C. Guyot[137], C. Gwenlan[121], C.B. Gwilliam[76], A. Haas[111], C. Haber[16], H.K. Hadavand[8], N. Haddad[136e], A. Hadef[87], S. Hageböck[23], M. Hagihara[165], Z. Hajduk[41], H. Hakobyan[181,*], M. Haleem[44], J. Haley[115], G. Halladjian[92], G.D. Hallewell[87], K. Hamacher[179], P. Hamal[116], K. Hamano[173], A. Hamilton[148a], G.N. Hamity[142], P.G. Hamnett[44], L. Han[59], K. Hanagaki[68,t], K. Hanawa[158], M. Hance[138], B. Haney[123], P. Hanke[60a], R. Hanna[137], J.B. Hansen[38], J.D. Hansen[38], M.C. Hansen[23], P.H. Hansen[38], K. Hara[165], A.S. Hard[177], T. Harenberg[179], F. Hariri[118], S. Harkusha[94], R.D. Harrington[48], P.F. Harrison[174], F. Hartjes[108], N.M. Hartmann[101], M. Hasegawa[69], Y. Hasegawa[143], A. Hasib[114], S. Hassani[137], S. Haug[18], R. Hauser[92], L. Hauswald[46], M. Havranek[128], C.M. Hawkes[19], R.J. Hawkings[32], D. Hayakawa[160], D. Hayden[92], C.P. Hays[121], J.M. Hays[78], H.S. Hayward[76], S.J. Haywood[132], S.J. Head[19], T. Heck[85], V. Hedberg[83], L. Heelan[8], S. Heim[123], T. Heim[16], B. Heinemann[16], J.J. Heinrich[101], L. Heinrich[111], C. Heinz[54], J. Hejbal[128], L. Helary[32], S. Hellman[149a,149b], C. Helsens[32], J. Henderson[121], R.C.W. Henderson[74], Y. Heng[177], S. Henkelmann[172], A.M. Henriques Correia[32], S. Henrot-Versille[118], G.H. Herbert[17], H. Herde[25], V. Herget[178], Y. Hernández Jiménez[171], G. Herten[50], R. Hertenberger[101], L. Hervas[32], G.G. Hesketh[80], N.P. Hessey[108], J.W. Hetherly[42], R. Hickling[78], E. Higón-Rodriguez[171], E. Hill[173], J.C. Hill[30], K.H. Hiller[44], S.J. Hillier[19], I. Hinchliffe[16], E. Hines[123], R.R. Hinman[16], M. Hirose[50], D. Hirschbuehl[179], J. Hobbs[151], N. Hod[164a], M.C. Hodgkinson[142], P. Hodgson[142], A. Hoecker[32], M.R. Hoeferkamp[106], F. Hoenig[101], D. Hohn[23], T.R. Holmes[16], M. Homann[45], T. Honda[68], T.M. Hong[126], B.H. Hooberman[170], W.H. Hopkins[117], Y. Horii[104], A.J. Horton[145], J-Y. Hostachy[57], S. Hou[154], A. Hoummada[136a], J. Howarth[44], J. Hoya[73], M. Hrabovsky[116], I. Hristova[17], J. Hrivnac[118], T. Hryn'ova[5], A. Hrynevich[95], C. Hsu[148c], P.J. Hsu[154,u], S.-C. Hsu[139], Q. Hu[59], S. Hu[141], Y. Huang[44], Z. Hubacek[129], F. Hubaut[87], F. Huegging[23], T.B. Huffman[121], E.W. Hughes[37], G. Hughes[74], M. Huhtinen[32], P. Huo[151], N. Huseynov[67,b], J. Huston[92], J. Huth[58], G. Iacobucci[51], G. Iakovidis[27], I. Ibragimov[144], L. Iconomidou-Fayard[118], E. Ideal[180], Z. Idrissi[136e], P. Iengo[32], O. Igonkina[108,v], T. Iizawa[175], Y. Ikegami[68], M. Ikeno[68], Y. Ilchenko[11,w], D. Iliadis[157], N. Ilic[146], T. Ince[102], G. Introzzi[122a,122b], P. Ioannou[9,*], M. Iodice[135a], K. Iordanidou[37], V. Ippolito[58], N. Ishijima[119], M. Ishino[158], M. Ishitsuka[160], R. Ishmukhametov[112], C. Issever[121], S. Istin[20a], F. Ito[165], J.M. Iturbe Ponce[86], R. Iuppa[163a,163b], W. Iwanski[64], H. Iwasaki[68], J.M. Izen[43], V. Izzo[105a], S. Jabbar[3], B. Jackson[123], P. Jackson[1], V. Jain[2], G. Jakel[179], K.B. Jakobi[85], K. Jakobs[50], S. Jakobsen[32], T. Jakoubek[128], D.O. Jamin[115], D.K. Jana[81], R. Jansky[64], J. Janssen[23], M. Janus[56], G. Jarlskog[83], N. Javadov[67,b], T. Javůrek[50], F. Jeanneau[137], L. Jeanty[16], G.-Y. Jeng[153], D. Jennens[90], P. Jenni[50,x],

JHEP04(2017)086

C. Jeske[174], S. Jézéquel[5], H. Ji[177], J. Jia[151], H. Jiang[66], Y. Jiang[59], S. Jiggins[80], J. Jimenez Pena[171], S. Jin[35a], A. Jinaru[28b], O. Jinnouchi[160], H. Jivan[148c], P. Johansson[142], K.A. Johns[7], W.J. Johnson[139], K. Jon-And[149a,149b], G. Jones[174], R.W.L. Jones[74], S. Jones[7], T.J. Jones[76], J. Jongmanns[60a], P.M. Jorge[127a,127b], J. Jovicevic[164a], X. Ju[177], A. Juste Rozas[13,s], M.K. Köhler[176], A. Kaczmarska[41], M. Kado[118], H. Kagan[112], M. Kagan[146], S.J. Kahn[87], T. Kaji[175], E. Kajomovitz[47], C.W. Kalderon[121], A. Kaluza[85], S. Kama[42], A. Kamenshchikov[131], N. Kanaya[158], S. Kaneti[30], L. Kanjir[77], V.A. Kantserov[99], J. Kanzaki[68], B. Kaplan[111], L.S. Kaplan[177], A. Kapliy[33], D. Kar[148c], K. Karakostas[10], A. Karamaoun[3], N. Karastathis[10], M.J. Kareem[56], E. Karentzos[10], M. Karnevskiy[85], S.N. Karpov[67], Z.M. Karpova[67], K. Karthik[111], V. Kartvelishvili[74], A.N. Karyukhin[131], K. Kasahara[165], L. Kashif[177], R.D. Kass[112], A. Kastanas[15], Y. Kataoka[158], C. Kato[158], A. Katre[51], J. Katzy[44], K. Kawade[104], K. Kawagoe[72], T. Kawamoto[158], G. Kawamura[56], V.F. Kazanin[110,c], R. Keeler[173], R. Kehoe[42], J.S. Keller[44], J.J. Kempster[79], H. Keoshkerian[162], O. Kepka[128], B.P. Kerševan[77], S. Kersten[179], R.A. Keyes[89], M. Khader[170], F. Khalil-zada[12], A. Khanov[115], A.G. Kharlamov[110,c], T. Kharlamova[110], T.J. Khoo[51], V. Khovanskiy[98], E. Khramov[67], J. Khubua[53b,y], S. Kido[69], C.R. Kilby[79], H.Y. Kim[8], S.H. Kim[165], Y.K. Kim[33], N. Kimura[157], O.M. Kind[17], B.T. King[76], M. King[171], J. Kirk[132], A.E. Kiryunin[102], T. Kishimoto[158], D. Kisielewska[40a], F. Kiss[50], K. Kiuchi[165], O. Kivernyk[137], E. Kladiva[147b], M.H. Klein[37], M. Klein[76], U. Klein[76], K. Kleinknecht[85], P. Klimek[109], A. Klimentov[27], R. Klingenberg[45], J.A. Klinger[142], T. Klioutchnikova[32], E.-E. Kluge[60a], P. Kluit[108], S. Kluth[102], J. Knapik[41], E. Kneringer[64], E.B.F.G. Knoops[87], A. Knue[55], A. Kobayashi[158], D. Kobayashi[160], T. Kobayashi[158], M. Kobel[46], M. Kocian[146], P. Kodys[130], N.M. Koehler[102], T. Koffas[31], E. Koffeman[108], T. Koi[146], H. Kolanoski[17], M. Kolb[60b], I. Koletsou[5], A.A. Komar[97,*], Y. Komori[158], T. Kondo[68], N. Kondrashova[44], K. Köneke[50], A.C. König[107], T. Kono[68,z], R. Konoplich[111,aa], N. Konstantinidis[80], R. Kopeliansky[63], S. Koperny[40a], L. Köpke[85], A.K. Kopp[50], K. Korcyl[41], K. Kordas[157], A. Korn[80], A.A. Korol[110,c], I. Korolkov[13], E.V. Korolkova[142], O. Kortner[102], S. Kortner[102], T. Kosek[130], V.V. Kostyukhin[23], A. Kotwal[47], A. Kourkoumeli-Charalampidi[122a,122b], C. Kourkoumelis[9], V. Kouskoura[27], A.B. Kowalewska[41], R. Kowalewski[173], T.Z. Kowalski[40a], C. Kozakai[158], W. Kozanecki[137], A.S. Kozhin[131], V.A. Kramarenko[100], G. Kramberger[77], D. Krasnopevtsev[99], M.W. Krasny[82], A. Krasznahorkay[32], A. Kravchenko[27], M. Kretz[60c], J. Kretzschmar[76], K. Kreutzfeldt[54], P. Krieger[162], K. Krizka[33], K. Kroeninger[45], H. Kroha[102], J. Kroll[123], J. Kroseberg[23], J. Krstic[14], U. Kruchonak[67], H. Krüger[23], N. Krumnack[66], M.C. Kruse[47], M. Kruskal[24], T. Kubota[90], H. Kucuk[80], S. Kuday[4b], J.T. Kuechler[179], S. Kuehn[50], A. Kugel[60c], F. Kuger[178], A. Kuhl[138], T. Kuhl[44], V. Kukhtin[67], R. Kukla[137], Y. Kulchitsky[94], S. Kuleshov[34b], M. Kuna[133a,133b], T. Kunigo[70], A. Kupco[128], H. Kurashige[69], Y.A. Kurochkin[94], V. Kus[128], E.S. Kuwertz[173], M. Kuze[160], J. Kvita[116], T. Kwan[173], D. Kyriazopoulos[142], A. La Rosa[102], J.L. La Rosa Navarro[26d], L. La Rotonda[39a,39b], C. Lacasta[171], F. Lacava[133a,133b], J. Lacey[31], H. Lacker[17], D. Lacour[82], V.R. Lacuesta[171], E. Ladygin[67], R. Lafaye[5], B. Laforge[82], T. Lagouri[180], S. Lai[56], S. Lammers[63], W. Lampl[7], E. Lançon[137], U. Landgraf[50], M.P.J. Landon[78], M.C. Lanfermann[51], V.S. Lang[60a], J.C. Lange[13], A.J. Lankford[167], F. Lanni[27], K. Lantzsch[23], A. Lanza[122a], S. Laplace[82], C. Lapoire[32], J.F. Laporte[137], T. Lari[93a], F. Lasagni Manghi[22a,22b], M. Lassnig[32], P. Laurelli[49], W. Lavrijsen[16], A.T. Law[138], P. Laycock[76], T. Lazovich[58], M. Lazzaroni[93a,93b], B. Le[90], O. Le Dortz[82], E. Le Guirriec[87], E.P. Le Quilleuc[137], M. LeBlanc[173], T. LeCompte[6], F. Ledroit-Guillon[57], C.A. Lee[27], S.C. Lee[154], L. Lee[1], B. Lefebvre[89], G. Lefebvre[82], M. Lefebvre[173], F. Legger[101], C. Leggett[16], A. Lehan[76], G. Lehmann Miotto[32], X. Lei[7], W.A. Leight[31], A.G. Leister[180], M.A.L. Leite[26d], R. Leitner[130], D. Lellouch[176], B. Lemmer[56], K.J.C. Leney[80], T. Lenz[23], B. Lenzi[32], R. Leone[7], S. Leone[125a,125b], C. Leonidopoulos[48], S. Leontsinis[10], G. Lerner[152], C. Leroy[96], A.A.J. Lesage[137], C.G. Lester[30], M. Levchenko[124], J. Levêque[5], D. Levin[91], L.J. Levinson[176], M. Levy[19], D. Lewis[78], A.M. Leyko[23], M. Leyton[43], B. Li[59,p], C. Li[59], H. Li[151], H.L. Li[33], L. Li[47], L. Li[141], Q. Li[35a], S. Li[47], X. Li[86], Y. Li[144], Z. Liang[35a], B. Liberti[134a], A. Liblong[162], P. Lichard[32], K. Lie[170], J. Liebal[23], W. Liebig[15], A. Limosani[153], S.C. Lin[154,ab], T.H. Lin[85], B.E. Lindquist[151], A.E. Lionti[51], E. Lipeles[123],

JHEP04(2017)086

A. Lipniacka[15], M. Lisovyi[60b], T.M. Liss[170], A. Lister[172], A.M. Litke[138], B. Liu[154,ac], D. Liu[154], H. Liu[91], H. Liu[27], J. Liu[87], J.B. Liu[59], K. Liu[87], L. Liu[170], M. Liu[47], M. Liu[59], Y.L. Liu[59], Y. Liu[59], M. Livan[122a,122b], A. Lleres[57], J. Llorente Merino[35a], S.L. Lloyd[78], F. Lo Sterzo[154], E.M. Lobodzinska[44], P. Loch[7], W.S. Lockman[138], F.K. Loebinger[86], K.M. Loew[25], A. Loginov[180,*], T. Lohse[17], K. Lohwasser[44], M. Lokajicek[128], B.A. Long[24], J.D. Long[170], R.E. Long[74], L. Longo[75a,75b], K.A. Looper[112], J.A. López[34b], D. Lopez Mateos[58], B. Lopez Paredes[142], I. Lopez Paz[13], A. Lopez Solis[82], J. Lorenz[101], N. Lorenzo Martinez[63], M. Losada[21], P.J. Lösel[101], X. Lou[35a], A. Lounis[118], J. Love[6], P.A. Love[74], H. Lu[62a], N. Lu[91], H.J. Lubatti[139], C. Luci[133a,133b], A. Lucotte[57], C. Luedtke[50], F. Luehring[63], W. Lukas[64], L. Luminari[133a], O. Lundberg[149a,149b], B. Lund-Jensen[150], P.M. Luzi[82], D. Lynn[27], R. Lysak[128], E. Lytken[83], V. Lyubushkin[67], H. Ma[27], L.L. Ma[140], Y. Ma[140], G. Maccarrone[49], A. Macchiolo[102], C.M. Macdonald[142], B. Maček[77], J. Machado Miguens[123,127b], D. Madaffari[87], R. Madar[36], H.J. Maddocks[169], W.F. Mader[46], A. Madsen[44], J. Maeda[69], S. Maeland[15], T. Maeno[27], A. Maevskiy[100], E. Magradze[56], J. Mahlstedt[108], C. Maiani[118], C. Maidantchik[26a], A.A. Maier[102], T. Maier[101], A. Maio[127a,127b,127d], S. Majewski[117], Y. Makida[68], N. Makovec[118], B. Malaescu[82], Pa. Malecki[41], V.P. Maleev[124], F. Malek[57], U. Mallik[65], D. Malon[6], C. Malone[146], C. Malone[30], S. Maltezos[10], S. Malyukov[32], J. Mamuzic[171], G. Mancini[49], L. Mandelli[93a], I. Mandić[77], J. Maneira[127a,127b], L. Manhaes de Andrade Filho[26b], J. Manjarres Ramos[164b], A. Mann[101], A. Manousos[32], B. Mansoulie[137], J.D. Mansour[35a], R. Mantifel[89], M. Mantoani[56], S. Manzoni[93a,93b], L. Mapelli[32], G. Marceca[29], L. March[51], G. Marchiori[82], M. Marcisovsky[128], M. Marjanovic[14], D.E. Marley[91], F. Marroquim[26a], S.P. Marsden[86], Z. Marshall[16], S. Marti-Garcia[171], B. Martin[92], T.A. Martin[174], V.J. Martin[48], B. Martin dit Latour[15], M. Martinez[13,s], V.I. Martinez Outschoorn[170], S. Martin-Haugh[132], V.S. Martoiu[28b], A.C. Martyniuk[80], A. Marzin[32], L. Masetti[85], T. Mashimo[158], R. Mashinistov[97], J. Masik[86], A.L. Maslennikov[110,c], I. Massa[22a,22b], L. Massa[22a,22b], P. Mastrandrea[5], A. Mastroberardino[39a,39b], T. Masubuchi[158], P. Mättig[179], J. Mattmann[85], J. Maurer[28b], S.J. Maxfield[76], D.A. Maximov[110,c], R. Mazini[154], S.M. Mazza[93a,93b], N.C. Mc Fadden[106], G. Mc Goldrick[162], S.P. Mc Kee[91], A. McCarn[91], R.L. McCarthy[151], T.G. McCarthy[102], L.I. McClymont[80], E.F. McDonald[90], J.A. Mcfayden[80], G. Mchedlidze[56], S.J. McMahon[132], R.A. McPherson[173,m], M. Medinnis[44], S. Meehan[139], S. Mehlhase[101], A. Mehta[76], K. Meier[60a], C. Meineck[101], B. Meirose[43], D. Melini[171], B.R. Mellado Garcia[148c], M. Melo[147a], F. Meloni[18], X. Meng[91], A. Mengarelli[22a,22b], S. Menke[102], E. Meoni[166], S. Mergelmeyer[17], P. Mermod[51], L. Merola[105a,105b], C. Meroni[93a], F.S. Merritt[33], A. Messina[133a,133b], J. Metcalfe[6], A.S. Mete[167], C. Meyer[85], C. Meyer[123], J-P. Meyer[137], J. Meyer[108], H. Meyer Zu Theenhausen[60a], F. Miano[152], R.P. Middleton[132], S. Miglioranzi[52a,52b], L. Mijović[48], G. Mikenberg[176], M. Mikestikova[128], M. Mikuž[77], M. Milesi[90], A. Milic[64], D.W. Miller[33], C. Mills[48], A. Milov[176], D.A. Milstead[149a,149b], A.A. Minaenko[131], Y. Minami[158], I.A. Minashvili[67], A.I. Mincer[111], B. Mindur[40a], M. Mineev[67], Y. Minegishi[158], Y. Ming[177], L.M. Mir[13], K.P. Mistry[123], T. Mitani[175], J. Mitrevski[101], V.A. Mitsou[171], A. Miucci[18], P.S. Miyagawa[142], J.U. Mjörnmark[83], M. Mlynarikova[130], T. Moa[149a,149b], K. Mochizuki[96], S. Mohapatra[37], S. Molander[149a,149b], R. Moles-Valls[23], R. Monden[70], M.C. Mondragon[92], K. Mönig[44], J. Monk[38], E. Monnier[87], A. Montalbano[151], J. Montejo Berlingen[32], F. Monticelli[73], S. Monzani[93a,93b], R.W. Moore[3], N. Morange[118], D. Moreno[21], M. Moreno Llácer[56], P. Morettini[52a], S. Morgenstern[32], D. Mori[145], T. Mori[158], M. Morii[58], M. Morinaga[158], V. Morisbak[120], S. Moritz[85], A.K. Morley[153], G. Mornacchi[32], J.D. Morris[78], S.S. Mortensen[38], L. Morvaj[151], M. Mosidze[53b], J. Moss[146,ad], K. Motohashi[160], R. Mount[146], E. Mountricha[27], E.J.W. Moyse[88], S. Muanza[87], R.D. Mudd[19], F. Mueller[102], J. Mueller[126], R.S.P. Mueller[101], T. Mueller[30], D. Muenstermann[74], P. Mullen[55], G.A. Mullier[18], F.J. Munoz Sanchez[86], J.A. Murillo Quijada[19], W.J. Murray[174,132], H. Musheghyan[56], M. Muškinja[77], A.G. Myagkov[131,ae], M. Myska[129], B.P. Nachman[146], O. Nackenhorst[51], K. Nagai[121], R. Nagai[68,z], K. Nagano[68], Y. Nagasaka[61], K. Nagata[165], M. Nagel[50], E. Nagy[87], A.M. Nairz[32], Y. Nakahama[104], K. Nakamura[68], T. Nakamura[158], I. Nakano[113], R.F. Naranjo Garcia[44], R. Narayan[11], D.I. Narrias Villar[60a], I. Naryshkin[124], T. Naumann[44],

G. Navarro[21], R. Nayyar[7], H.A. Neal[91], P.Yu. Nechaeva[97], T.J. Neep[86], A. Negri[122a,122b], M. Negrini[22a], S. Nektarijevic[107], C. Nellist[118], A. Nelson[167], S. Nemecek[128], P. Nemethy[111], A.A. Nepomuceno[26a], M. Nessi[32,af], M.S. Neubauer[170], M. Neumann[179], R.M. Neves[111], P. Nevski[27], P.R. Newman[19], D.H. Nguyen[6], T. Nguyen Manh[96], R.B. Nickerson[121], R. Nicolaidou[137], J. Nielsen[138], A. Nikiforov[17], V. Nikolaenko[131,ae], I. Nikolic-Audit[82], K. Nikolopoulos[19], J.K. Nilsen[120], P. Nilsson[27], Y. Ninomiya[158], A. Nisati[133a], R. Nisius[102], T. Nobe[158], M. Nomachi[119], I. Nomidis[31], T. Nooney[78], S. Norberg[114], M. Nordberg[32], N. Norjoharuddeen[121], O. Novgorodova[46], S. Nowak[102], M. Nozaki[68], L. Nozka[116], K. Ntekas[167], E. Nurse[80], F. Nuti[90], F. O'grady[7], D.C. O'Neil[145], A.A. O'Rourke[44], V. O'Shea[55], F.G. Oakham[31,d], H. Oberlack[102], T. Obermann[23], J. Ocariz[82], A. Ochi[69], I. Ochoa[37], J.P. Ochoa-Ricoux[34a], S. Oda[72], S. Odaka[68], H. Ogren[63], A. Oh[86], S.H. Oh[47], C.C. Ohm[16], H. Ohman[169], H. Oide[32], H. Okawa[165], Y. Okumura[158], T. Okuyama[68], A. Olariu[28b], L.F. Oleiro Seabra[127a], S.A. Olivares Pino[48], D. Oliveira Damazio[27], A. Olszewski[41], J. Olszowska[41], A. Onofre[127a,127e], K. Onogi[104], P.U.E. Onyisi[11,w], M.J. Oreglia[33], Y. Oren[156], D. Orestano[135a,135b], N. Orlando[62b], R.S. Orr[162], B. Osculati[52a,52b,*], R. Ospanov[86], G. Otero y Garzon[29], H. Otono[72], M. Ouchrif[136d], F. Ould-Saada[120], A. Ouraou[137], K.P. Oussoren[108], Q. Ouyang[35a], M. Owen[55], R.E. Owen[19], V.E. Ozcan[20a], N. Ozturk[8], K. Pachal[145], A. Pacheco Pages[13], L. Pacheco Rodriguez[137], C. Padilla Aranda[13], M. Pagáčová[50], S. Pagan Griso[16], M. Paganini[180], F. Paige[27], P. Pais[88], K. Pajchel[120], G. Palacino[164b], S. Palazzo[39a,39b], S. Palestini[32], M. Palka[40b], D. Pallin[36], E.St. Panagiotopoulou[10], C.E. Pandini[82], J.G. Panduro Vazquez[79], P. Pani[149a,149b], S. Panitkin[27], D. Pantea[28b], L. Paolozzi[51], Th.D. Papadopoulou[10], K. Papageorgiou[157], A. Paramonov[6], D. Paredes Hernandez[180], A.J. Parker[74], M.A. Parker[30], K.A. Parker[142], F. Parodi[52a,52b], J.A. Parsons[37], U. Parzefall[50], V.R. Pascuzzi[162], E. Pasqualucci[133a], S. Passaggio[52a], Fr. Pastore[79], G. Pásztor[31,ag], S. Pataraia[179], J.R. Pater[86], T. Pauly[32], J. Pearce[173], B. Pearson[114], L.E. Pedersen[38], M. Pedersen[120], S. Pedraza Lopez[171], R. Pedro[127a,127b], S.V. Peleganchuk[110,c], O. Penc[128], C. Peng[35a], H. Peng[59], J. Penwell[63], B.S. Peralva[26b], M.M. Perego[137], D.V. Perepelitsa[27], E. Perez Codina[164a], L. Perini[93a,93b], H. Pernegger[32], S. Perrella[105a,105b], R. Peschke[44], V.D. Peshekhonov[67], K. Peters[44], R.F.Y. Peters[86], B.A. Petersen[32], T.C. Petersen[38], E. Petit[57], A. Petridis[1], C. Petridou[157], P. Petroff[118], E. Petrolo[133a], M. Petrov[121], F. Petrucci[135a,135b], N.E. Pettersson[88], A. Peyaud[137], R. Pezoa[34b], P.W. Phillips[132], G. Piacquadio[146,ah], E. Pianori[174], A. Picazio[88], E. Piccaro[78], M. Piccinini[22a,22b], M.A. Pickering[121], R. Piegaia[29], J.E. Pilcher[33], A.D. Pilkington[86], A.W.J. Pin[86], M. Pinamonti[168a,168c,ai], J.L. Pinfold[3], A. Pingel[38], S. Pires[82], H. Pirumov[44], M. Pitt[176], L. Plazak[147a], M.-A. Pleier[27], V. Pleskot[85], E. Plotnikova[67], P. Plucinski[92], D. Pluth[66], R. Poettgen[149a,149b], L. Poggioli[118], D. Pohl[23], G. Polesello[122a], A. Poley[44], A. Policicchio[39a,39b], R. Polifka[162], A. Polini[22a], C.S. Pollard[55], V. Polychronakos[27], K. Pommès[32], L. Pontecorvo[133a], B.G. Pope[92], G.A. Popeneciu[28c], A. Poppleton[32], S. Pospisil[129], K. Potamianos[16], I.N. Potrap[67], C.J. Potter[30], C.T. Potter[117], G. Poulard[32], J. Poveda[32], V. Pozdnyakov[67], M.E. Pozo Astigarraga[32], P. Pralavorio[87], A. Pranko[16], S. Prell[66], D. Price[86], L.E. Price[6], M. Primavera[75a], S. Prince[89], K. Prokofiev[62c], F. Prokoshin[34b], S. Protopopescu[27], J. Proudfoot[6], M. Przybycien[40a], D. Puddu[135a,135b], M. Purohit[27,aj], P. Puzo[118], J. Qian[91], G. Qin[55], Y. Qin[86], A. Quadt[56], W.B. Quayle[168a,168b], M. Queitsch-Maitland[44], D. Quilty[55], S. Raddum[120], V. Radeka[27], V. Radescu[121], S.K. Radhakrishnan[151], P. Radloff[117], P. Rados[90], F. Ragusa[93a,93b], G. Rahal[182], J.A. Raine[86], S. Rajagopalan[27], M. Rammensee[32], C. Rangel-Smith[169], M.G. Ratti[93a,93b], F. Rauscher[101], S. Rave[85], T. Ravenscroft[55], I. Ravinovich[176], M. Raymond[32], A.L. Read[120], N.P. Readioff[76], M. Reale[75a,75b], D.M. Rebuzzi[122a,122b], A. Redelbach[178], G. Redlinger[27], R. Reece[138], R.G. Reed[148c], K. Reeves[43], L. Rehnisch[17], J. Reichert[123], A. Reiss[85], C. Rembser[32], H. Ren[35a], M. Rescigno[133a], S. Resconi[93a], O.L. Rezanova[110,c], P. Reznicek[130], R. Rezvani[96], R. Richter[102], S. Richter[80], E. Richter-Was[40b], O. Ricken[23], M. Ridel[82], P. Rieck[17], C.J. Riegel[179], J. Rieger[56], O. Rifki[114], M. Rijssenbeek[151], A. Rimoldi[122a,122b], M. Rimoldi[18], L. Rinaldi[22a], B. Ristić[51], E. Ritsch[32], I. Riu[13], F. Rizatdinova[115], E. Rizvi[78], C. Rizzi[13], S.H. Robertson[89,m], A. Robichaud-Veronneau[89], D. Robinson[30], J.E.M. Robinson[44], A. Robson[55], C. Roda[125a,125b], Y. Rodina[87,ak], A. Rodriguez Perez[13],

D. Rodriguez Rodriguez[171], S. Roe[32], C.S. Rogan[58], O. Røhne[120], A. Romaniouk[99], M. Romano[22a,22b], S.M. Romano Saez[36], E. Romero Adam[171], N. Rompotis[139], M. Ronzani[50], L. Roos[82], E. Ros[171], S. Rosati[133a], K. Rosbach[50], P. Rose[138], N.-A. Rosien[56], V. Rossetti[149a,149b], E. Rossi[105a,105b], L.P. Rossi[52a], J.H.N. Rosten[30], R. Rosten[139], M. Rotaru[28b], I. Roth[176], J. Rothberg[139], D. Rousseau[118], A. Rozanov[87], Y. Rozen[155], X. Ruan[148c], F. Rubbo[146], M.S. Rudolph[162], F. Rühr[50], A. Ruiz-Martinez[31], Z. Rurikova[50], N.A. Rusakovich[67], A. Ruschke[101], H.L. Russell[139], J.P. Rutherfoord[7], N. Ruthmann[32], Y.F. Ryabov[124], M. Rybar[170], G. Rybkin[118], S. Ryu[6], A. Ryzhov[131], G.F. Rzehorz[56], A.F. Saavedra[153], G. Sabato[108], S. Sacerdoti[29], H.F-W. Sadrozinski[138], R. Sadykov[67], F. Safai Tehrani[133a], P. Saha[109], M. Sahinsoy[60a], M. Saimpert[137], T. Saito[158], H. Sakamoto[158], Y. Sakurai[175], G. Salamanna[135a,135b], A. Salamon[134a,134b], J.E. Salazar Loyola[34b], D. Salek[108], P.H. Sales De Bruin[139], D. Salihagic[102], A. Salnikov[146], J. Salt[171], D. Salvatore[39a,39b], F. Salvatore[152], A. Salvucci[62a,62b,62c], A. Salzburger[32], D. Sammel[50], D. Sampsonidis[157], J. Sánchez[171], V. Sanchez Martinez[171], A. Sanchez Pineda[105a,105b], H. Sandaker[120], R.L. Sandbach[78], M. Sandhoff[179], C. Sandoval[21], D.P.C. Sankey[132], M. Sannino[52a,52b], A. Sansoni[49], C. Santoni[36], R. Santonico[134a,134b], H. Santos[127a], I. Santoyo Castillo[152], K. Sapp[126], A. Sapronov[67], J.G. Saraiva[127a,127d], B. Sarrazin[23], O. Sasaki[68], K. Sato[165], E. Sauvan[5], G. Savage[79], P. Savard[162,d], N. Savic[102], C. Sawyer[132], L. Sawyer[81,r], J. Saxon[33], C. Sbarra[22a], A. Sbrizzi[22a,22b], T. Scanlon[80], D.A. Scannicchio[167], M. Scarcella[153], V. Scarfone[39a,39b], J. Schaarschmidt[176], P. Schacht[102], B.M. Schachtner[101], D. Schaefer[32], L. Schaefer[123], R. Schaefer[44], J. Schaeffer[85], S. Schaepe[23], S. Schaetzel[60b], U. Schäfer[85], A.C. Schaffer[118], D. Schaile[101], R.D. Schamberger[151], V. Scharf[60a], V.A. Schegelsky[124], D. Scheirich[130], M. Schernau[167], C. Schiavi[52a,52b], S. Schier[138], C. Schillo[50], M. Schioppa[39a,39b], S. Schlenker[32], K.R. Schmidt-Sommerfeld[102], K. Schmieden[32], C. Schmitt[85], S. Schmitt[44], S. Schmitz[85], B. Schneider[164a], U. Schnoor[50], L. Schoeffel[137], A. Schoening[60b], B.D. Schoenrock[92], E. Schopf[23], M. Schott[85], J.F.P. Schouwenberg[107], J. Schovancova[8], S. Schramm[51], M. Schreyer[178], N. Schuh[85], A. Schulte[85], M.J. Schultens[23], H.-C. Schultz-Coulon[60a], H. Schulz[17], M. Schumacher[50], B.A. Schumm[138], Ph. Schune[137], A. Schwartzman[146], T.A. Schwarz[91], H. Schweiger[86], Ph. Schwemling[137], R. Schwienhorst[92], J. Schwindling[137], T. Schwindt[23], G. Sciolla[25], F. Scuri[125a,125b], F. Scutti[90], J. Searcy[91], P. Seema[23], S.C. Seidel[106], A. Seiden[138], F. Seifert[129], J.M. Seixas[26a], G. Sekhniaidze[105a], K. Sekhon[91], S.J. Sekula[42], D.M. Seliverstov[124,*], N. Semprini-Cesari[22a,22b], C. Serfon[120], L. Serin[118], L. Serkin[168a,168b], M. Sessa[135a,135b], R. Seuster[173], H. Severini[114], T. Sfiligoj[77], F. Sforza[32], A. Sfyrla[51], E. Shabalina[56], N.W. Shaikh[149a,149b], L.Y. Shan[35a], R. Shang[170], J.T. Shank[24], M. Shapiro[16], P.B. Shatalov[98], K. Shaw[168a,168b], S.M. Shaw[86], A. Shcherbakova[149a,149b], C.Y. Shehu[152], P. Sherwood[80], L. Shi[154,al], S. Shimizu[69], C.O. Shimmin[167], M. Shimojima[103], S. Shirabe[72], M. Shiyakova[67,am], A. Shmeleva[97], D. Shoaleh Saadi[96], M.J. Shochet[33], S. Shojaii[93a,93b], D.R. Shope[114], S. Shrestha[112], E. Shulga[99], M.A. Shupe[7], P. Sicho[128], A.M. Sickles[170], P.E. Sidebo[150], O. Sidiropoulou[178], D. Sidorov[115], A. Sidoti[22a,22b], F. Siegert[46], Dj. Sijacki[14], J. Silva[127a,127d], S.B. Silverstein[149a], V. Simak[129], Lj. Simic[14], S. Simion[118], E. Simioni[85], B. Simmons[80], D. Simon[36], M. Simon[85], P. Sinervo[162], N.B. Sinev[117], M. Sioli[22a,22b], G. Siragusa[178], S.Yu. Sivoklokov[100], J. Sjölin[149a,149b], M.B. Skinner[74], H.P. Skottowe[58], P. Skubic[114], M. Slater[19], T. Slavicek[129], M. Slawinska[108], K. Sliwa[166], R. Slovak[130], V. Smakhtin[176], B.H. Smart[5], L. Smestad[15], J. Smiesko[147a], S.Yu. Smirnov[99], Y. Smirnov[99], L.N. Smirnova[100,an], O. Smirnova[83], M.N.K. Smith[37], R.W. Smith[37], M. Smizanska[74], K. Smolek[129], A.A. Snesarev[97], I.M. Snyder[117], S. Snyder[27], R. Sobie[173,m], F. Socher[46], A. Soffer[156], D.A. Soh[154], G. Sokhrannyi[77], C.A. Solans Sanchez[32], M. Solar[129], E.Yu. Soldatov[99], U. Soldevila[171], A.A. Solodkov[131], A. Soloshenko[67], O.V. Solovyanov[131], V. Solovyev[124], P. Sommer[50], H. Son[166], H.Y. Song[59,ao], A. Sood[16], A. Sopczak[129], V. Sopko[129], V. Sorin[13], D. Sosa[60b], C.L. Sotiropoulou[125a,125b], R. Soualah[168a,168c], A.M. Soukharev[110,c], D. South[44], B.C. Sowden[79], S. Spagnolo[75a,75b], M. Spalla[125a,125b], M. Spangenberg[174], F. Spanò[79], D. Sperlich[17], F. Spettel[102], R. Spighi[22a], G. Spigo[32], L.A. Spiller[90], M. Spousta[130], R.D. St. Denis[55,*], A. Stabile[93a], R. Stamen[60a], S. Stamm[17], E. Stanecka[41], R.W. Stanek[6], C. Stanescu[135a], M. Stanescu-Bellu[44], M.M. Stanitzki[44],

S. Stapnes[120], E.A. Starchenko[131], G.H. Stark[33], J. Stark[57], P. Staroba[128], P. Starovoitov[60a], S. Stärz[32], R. Staszewski[41], P. Steinberg[27], B. Stelzer[145], H.J. Stelzer[32], O. Stelzer-Chilton[164a], H. Stenzel[54], G.A. Stewart[55], J.A. Stillings[23], M.C. Stockton[89], M. Stoebe[89], G. Stoicea[28b], P. Stolte[56], S. Stonjek[102], A.R. Stradling[8], A. Straessner[46], M.E. Stramaglia[18], J. Strandberg[150], S. Strandberg[149a,149b], A. Strandlie[120], M. Strauss[114], P. Strizenec[147b], R. Ströhmer[178], D.M. Strom[117], R. Stroynowski[42], A. Strubig[107], S.A. Stucci[27], B. Stugu[15], N.A. Styles[44], D. Su[146], J. Su[126], S. Suchek[60a], Y. Sugaya[119], M. Suk[129], V.V. Sulin[97], S. Sultansoy[4c], T. Sumida[70], S. Sun[58], X. Sun[35a], J.E. Sundermann[50], K. Suruliz[152], G. Susinno[39a,39b], M.R. Sutton[152], S. Suzuki[68], M. Svatos[128], M. Swiatlowski[33], I. Sykora[147a], T. Sykora[130], D. Ta[50], C. Taccini[135a,135b], K. Tackmann[44], J. Taenzer[162], A. Taffard[167], R. Tafirout[164a], N. Taiblum[156], H. Takai[27], R. Takashima[71], T. Takeshita[143], Y. Takubo[68], M. Talby[87], A.A. Talyshev[110,c], K.G. Tan[90], J. Tanaka[158], M. Tanaka[160], R. Tanaka[118], S. Tanaka[68], R. Tanioka[69], B.B. Tannenwald[112], S. Tapia Araya[34b], S. Tapprogge[85], S. Tarem[155], G.F. Tartarelli[93a], P. Tas[130], M. Tasevsky[128], T. Tashiro[70], E. Tassi[39a,39b], A. Tavares Delgado[127a,127b], Y. Tayalati[136e], A.C. Taylor[106], G.N. Taylor[90], P.T.E. Taylor[90], W. Taylor[164b], F.A. Teischinger[32], P. Teixeira-Dias[79], K.K. Temming[50], D. Temple[145], H. Ten Kate[32], P.K. Teng[154], J.J. Teoh[119], F. Tepel[179], S. Terada[68], K. Terashi[158], J. Terron[84], S. Terzo[13], M. Testa[49], R.J. Teuscher[162,m], T. Theveneaux-Pelzer[87], J.P. Thomas[19], J. Thomas-Wilsker[79], E.N. Thompson[37], P.D. Thompson[19], A.S. Thompson[55], L.A. Thomsen[180], E. Thomson[123], M.J. Tibbetts[16], R.E. Ticse Torres[87], V.O. Tikhomirov[97,ap], Yu.A. Tikhonov[110,c], S. Timoshenko[99], P. Tipton[180], S. Tisserant[87], K. Todome[160], T. Todorov[5,*], S. Todorova-Nova[130], J. Tojo[72], S. Tokár[147a], K. Tokushuku[68], E. Tolley[58], L. Tomlinson[86], M. Tomoto[104], L. Tompkins[146,aq], K. Toms[106], B. Tong[58], P. Tornambe[50], E. Torrence[117], H. Torres[145], E. Torró Pastor[139], J. Toth[87,ar], F. Touchard[87], D.R. Tovey[142], T. Trefzger[178], A. Tricoli[27], I.M. Trigger[164a], S. Trincaz-Duvoid[82], M.F. Tripiana[13], W. Trischuk[162], B. Trocmé[57], A. Trofymov[44], C. Troncon[93a], M. Trottier-McDonald[16], M. Trovatelli[173], L. Truong[168a,168c], M. Trzebinski[41], A. Trzupek[41], J.C-L. Tseng[121], P.V. Tsiareshka[94], G. Tsipolitis[10], N. Tsirintanis[9], S. Tsiskaridze[13], V. Tsiskaridze[50], E.G. Tskhadadze[53a], K.M. Tsui[62a], I.I. Tsukerman[98], V. Tsulaia[16], S. Tsuno[68], D. Tsybychev[151], Y. Tu[62b], A. Tudorache[28b], V. Tudorache[28b], A.N. Tuna[58], S.A. Tupputi[22a,22b], S. Turchikhin[67], D. Turecek[129], D. Turgeman[176], R. Turra[93a,93b], P.M. Tuts[37], M. Tyndel[132], G. Ucchielli[22a,22b], I. Ueda[158], M. Ughetto[149a,149b], F. Ukegawa[165], G. Unal[32], A. Undrus[27], G. Unel[167], F.C. Ungaro[90], Y. Unno[68], C. Unverdorben[101], J. Urban[147b], P. Urquijo[90], P. Urrejola[85], G. Usai[8], L. Vacavant[87], V. Vacek[129], B. Vachon[89], C. Valderanis[101], E. Valdes Santurio[149a,149b], N. Valencic[108], S. Valentinetti[22a,22b], A. Valero[171], L. Valery[13], S. Valkar[130], J.A. Valls Ferrer[171], W. Van Den Wollenberg[108], P.C. Van Der Deijl[108], H. van der Graaf[108], N. van Eldik[155], P. van Gemmeren[6], J. Van Nieuwkoop[145], I. van Vulpen[108], M.C. van Woerden[32], M. Vanadia[133a,133b], W. Vandelli[32], R. Vanguri[123], A. Vaniachine[161], P. Vankov[108], G. Vardanyan[181], R. Vari[133a], E.W. Varnes[7], T. Varol[42], D. Varouchas[82], A. Vartapetian[8], K.E. Varvell[153], J.G. Vasquez[180], G.A. Vasquez[34b], F. Vazeille[36], T. Vazquez Schroeder[89], J. Veatch[56], V. Veeraraghavan[7], L.M. Veloce[162], F. Veloso[127a,127c], S. Veneziano[133a], A. Ventura[75a,75b], M. Venturi[173], N. Venturi[162], A. Venturini[25], V. Vercesi[122a], M. Verducci[133a,133b], W. Verkerke[108], J.C. Vermeulen[108], A. Vest[46,as], M.C. Vetterli[145,d], O. Viazlo[83], I. Vichou[170,*], T. Vickey[142], O.E. Vickey Boeriu[142], G.H.A. Viehhauser[121], S. Viel[16], L. Vigani[121], M. Villa[22a,22b], M. Villaplana Perez[93a,93b], E. Vilucchi[49], M.G. Vincter[31], V.B. Vinogradov[67], C. Vittori[22a,22b], I. Vivarelli[152], S. Vlachos[10], M. Vlasak[129], M. Vogel[179], P. Vokac[129], G. Volpi[125a,125b], M. Volpi[90], H. von der Schmitt[102], E. von Toerne[23], V. Vorobel[130], K. Vorobev[99], M. Vos[171], R. Voss[32], J.H. Vossebeld[76], N. Vranjes[14], M. Vranjes Milosavljevic[14], V. Vrba[128], M. Vreeswijk[108], R. Vuillermet[32], I. Vukotic[33], Z. Vykydal[129], P. Wagner[23], W. Wagner[179], H. Wahlberg[73], S. Wahrmund[46], J. Wakabayashi[104], J. Walder[74], R. Walker[101], W. Walkowiak[144], V. Wallangen[149a,149b], C. Wang[35b], C. Wang[140,87], F. Wang[177], H. Wang[16], H. Wang[42], J. Wang[44], J. Wang[153], K. Wang[89], R. Wang[6], S.M. Wang[154], T. Wang[23], T. Wang[37], W. Wang[59], X. Wang[180], C. Wanotayaroj[117], A. Warburton[89], C.P. Ward[30], D.R. Wardrope[80], A. Washbrook[48], P.M. Watkins[19],

JHEP04(2017)086

A.T. Watson[19], M.F. Watson[19], G. Watts[139], S. Watts[86], B.M. Waugh[80], S. Webb[85], M.S. Weber[18], S.W. Weber[178], S.A. Weber[31], J.S. Webster[6], A.R. Weidberg[121], B. Weinert[63], J. Weingarten[56], C. Weiser[50], H. Weits[108], P.S. Wells[32], T. Wenaus[27], T. Wengler[32], S. Wenig[32], N. Wermes[23], M. Werner[50], M.D. Werner[66], P. Werner[32], M. Wessels[60a], J. Wetter[166], K. Whalen[117], N.L. Whallon[139], A.M. Wharton[74], A. White[8], M.J. White[1], R. White[34b], D. Whiteson[167], F.J. Wickens[132], W. Wiedenmann[177], M. Wielers[132], C. Wiglesworth[38], L.A.M. Wiik-Fuchs[23], A. Wildauer[102], F. Wilk[86], H.G. Wilkens[32], H.H. Williams[123], S. Williams[108], C. Willis[92], S. Willocq[88], J.A. Wilson[19], I. Wingerter-Seez[5], F. Winklmeier[117], O.J. Winston[152], B.T. Winter[23], M. Wittgen[146], J. Wittkowski[101], T.M.H. Wolf[108], M.W. Wolter[41], H. Wolters[127a,127c], S.D. Worm[132], B.K. Wosiek[41], J. Wotschack[32], M.J. Woudstra[86], K.W. Wozniak[41], M. Wu[57], M. Wu[33], S.L. Wu[177], X. Wu[51], Y. Wu[91], T.R. Wyatt[86], B.M. Wynne[48], S. Xella[38], D. Xu[35a], L. Xu[27], B. Yabsley[153], S. Yacoob[148a], D. Yamaguchi[160], Y. Yamaguchi[119], A. Yamamoto[68], S. Yamamoto[158], T. Yamanaka[158], K. Yamauchi[104], Y. Yamazaki[69], Z. Yan[24], H. Yang[141], H. Yang[177], Y. Yang[154], Z. Yang[15], W-M. Yao[16], Y.C. Yap[82], Y. Yasu[68], E. Yatsenko[5], K.H. Yau Wong[23], J. Ye[42], S. Ye[27], I. Yeletskikh[67], A.L. Yen[58], E. Yildirim[85], K. Yorita[175], R. Yoshida[6], K. Yoshihara[123], C. Young[146], C.J.S. Young[32], S. Youssef[24], D.R. Yu[16], J. Yu[8], J.M. Yu[91], J. Yu[66], L. Yuan[69], S.P.Y. Yuen[23], I. Yusuff[30,at], B. Zabinski[41], R. Zaidan[65], A.M. Zaitsev[131,ae], N. Zakharchuk[44], J. Zalieckas[15], A. Zaman[151], S. Zambito[58], L. Zanello[133a,133b], D. Zanzi[90], C. Zeitnitz[179], M. Zeman[129], A. Zemla[40a], J.C. Zeng[170], Q. Zeng[146], K. Zengel[25], O. Zenin[131], T. Ženiš[147a], D. Zerwas[118], D. Zhang[91], F. Zhang[177], G. Zhang[59,ao], H. Zhang[35b], J. Zhang[6], L. Zhang[50], R. Zhang[23], R. Zhang[59,au], X. Zhang[140], Z. Zhang[118], X. Zhao[42], Y. Zhao[140], Z. Zhao[59], A. Zhemchugov[67], J. Zhong[121], B. Zhou[91], C. Zhou[177], L. Zhou[37], L. Zhou[42], M. Zhou[151], N. Zhou[35c], C.G. Zhu[140], H. Zhu[35a], J. Zhu[91], Y. Zhu[59], X. Zhuang[35a], K. Zhukov[97], A. Zibell[178], D. Zieminska[63], N.I. Zimine[67], C. Zimmermann[85], S. Zimmermann[50], Z. Zinonos[56], M. Zinser[85], M. Ziolkowski[144], L. Živković[14], G. Zobernig[177], A. Zoccoli[22a,22b], M. zur Nedden[17], L. Zwalinski[32]

1 *Department of Physics, University of Adelaide, Adelaide, Australia*
2 *Physics Department, SUNY Albany, Albany NY, United States of America*
3 *Department of Physics, University of Alberta, Edmonton AB, Canada*
4 *[(a)] Department of Physics, Ankara University, Ankara; [(b)] Istanbul Aydin University, Istanbul; [(c)] Division of Physics, TOBB University of Economics and Technology, Ankara, Turkey*
5 *LAPP, CNRS/IN2P3 and Université Savoie Mont Blanc, Annecy-le-Vieux, France*
6 *High Energy Physics Division, Argonne National Laboratory, Argonne IL, United States of America*
7 *Department of Physics, University of Arizona, Tucson AZ, United States of America*
8 *Department of Physics, The University of Texas at Arlington, Arlington TX, United States of America*
9 *Physics Department, University of Athens, Athens, Greece*
10 *Physics Department, National Technical University of Athens, Zografou, Greece*
11 *Department of Physics, The University of Texas at Austin, Austin TX, United States of America*
12 *Institute of Physics, Azerbaijan Academy of Sciences, Baku, Azerbaijan*
13 *Institut de Física d'Altes Energies (IFAE), The Barcelona Institute of Science and Technology, Barcelona, Spain*
14 *Institute of Physics, University of Belgrade, Belgrade, Serbia*
15 *Department for Physics and Technology, University of Bergen, Bergen, Norway*
16 *Physics Division, Lawrence Berkeley National Laboratory and University of California, Berkeley CA, United States of America*
17 *Department of Physics, Humboldt University, Berlin, Germany*
18 *Albert Einstein Center for Fundamental Physics and Laboratory for High Energy Physics, University of Bern, Bern, Switzerland*
19 *School of Physics and Astronomy, University of Birmingham, Birmingham, United Kingdom*
20 *[(a)] Department of Physics, Bogazici University, Istanbul; [(b)] Department of Physics Engineering, Gaziantep University, Gaziantep; [(d)] Istanbul Bilgi University, Faculty of Engineering and Natural Sciences, Istanbul,Turkey; [(e)] Bahcesehir University, Faculty of Engineering and Natural Sciences, Istanbul, Turkey*

JHEP04(2017)086

21 Centro de Investigaciones, Universidad Antonio Narino, Bogota, Colombia
22 (a) INFN Sezione di Bologna; (b) Dipartimento di Fisica e Astronomia, Università di Bologna, Bologna, Italy
23 Physikalisches Institut, University of Bonn, Bonn, Germany
24 Department of Physics, Boston University, Boston MA, United States of America
25 Department of Physics, Brandeis University, Waltham MA, United States of America
26 (a) Universidade Federal do Rio De Janeiro COPPE/EE/IF, Rio de Janeiro; (b) Electrical Circuits Department, Federal University of Juiz de Fora (UFJF), Juiz de Fora; (c) Federal University of Sao Joao del Rei (UFSJ), Sao Joao del Rei; (d) Instituto de Fisica, Universidade de Sao Paulo, Sao Paulo, Brazil
27 Physics Department, Brookhaven National Laboratory, Upton NY, United States of America
28 (a) Transilvania University of Brasov, Brasov; (b) National Institute of Physics and Nuclear Engineering, Bucharest; (c) National Institute for Research and Development of Isotopic and Molecular Technologies, Physics Department, Cluj Napoca; (d) University Politehnica Bucharest, Bucharest; (e) West University in Timisoara, Timisoara, Romania
29 Departamento de Física, Universidad de Buenos Aires, Buenos Aires, Argentina
30 Cavendish Laboratory, University of Cambridge, Cambridge, United Kingdom
31 Department of Physics, Carleton University, Ottawa ON, Canada
32 CERN, Geneva, Switzerland
33 Enrico Fermi Institute, University of Chicago, Chicago IL, United States of America
34 (a) Departamento de Física, Pontificia Universidad Católica de Chile, Santiago; (b) Departamento de Física, Universidad Técnica Federico Santa María, Valparaíso, Chile
35 (a) Institute of High Energy Physics, Chinese Academy of Sciences, Beijing; (b) Department of Physics, Nanjing University, Jiangsu; (c) Physics Department, Tsinghua University, Beijing 100084, China
36 Laboratoire de Physique Corpusculaire, Clermont Université and Université Blaise Pascal and CNRS/IN2P3, Clermont-Ferrand, France
37 Nevis Laboratory, Columbia University, Irvington NY, United States of America
38 Niels Bohr Institute, University of Copenhagen, Kobenhavn, Denmark
39 (a) INFN Gruppo Collegato di Cosenza, Laboratori Nazionali di Frascati; (b) Dipartimento di Fisica, Università della Calabria, Rende, Italy
40 (a) AGH University of Science and Technology, Faculty of Physics and Applied Computer Science, Krakow; (b) Marian Smoluchowski Institute of Physics, Jagiellonian University, Krakow, Poland
41 Institute of Nuclear Physics Polish Academy of Sciences, Krakow, Poland
42 Physics Department, Southern Methodist University, Dallas TX, United States of America
43 Physics Department, University of Texas at Dallas, Richardson TX, United States of America
44 DESY, Hamburg and Zeuthen, Germany
45 Lehrstuhl für Experimentelle Physik IV, Technische Universität Dortmund, Dortmund, Germany
46 Institut für Kern- und Teilchenphysik, Technische Universität Dresden, Dresden, Germany
47 Department of Physics, Duke University, Durham NC, United States of America
48 SUPA — School of Physics and Astronomy, University of Edinburgh, Edinburgh, United Kingdom
49 INFN Laboratori Nazionali di Frascati, Frascati, Italy
50 Fakultät für Mathematik und Physik, Albert-Ludwigs-Universität, Freiburg, Germany
51 Section de Physique, Université de Genève, Geneva, Switzerland
52 (a) INFN Sezione di Genova; (b) Dipartimento di Fisica, Università di Genova, Genova, Italy
53 (a) E. Andronikashvili Institute of Physics, Iv. Javakhishvili Tbilisi State University, Tbilisi; (b) High Energy Physics Institute, Tbilisi State University, Tbilisi, Georgia
54 II Physikalisches Institut, Justus-Liebig-Universität Giessen, Giessen, Germany
55 SUPA - School of Physics and Astronomy, University of Glasgow, Glasgow, United Kingdom
56 II Physikalisches Institut, Georg-August-Universität, Göttingen, Germany
57 Laboratoire de Physique Subatomique et de Cosmologie, Université Grenoble-Alpes, CNRS/IN2P3, Grenoble, France
58 Laboratory for Particle Physics and Cosmology, Harvard University, Cambridge MA, United States of America
59 Department of Modern Physics, University of Science and Technology of China, Anhui, China

[60] [(a)] Kirchhoff-Institut für Physik, Ruprecht-Karls-Universität Heidelberg, Heidelberg; [(b)] Physikalisches Institut, Ruprecht-Karls-Universität Heidelberg, Heidelberg; [(c)] ZITI Institut für technische Informatik, Ruprecht-Karls-Universität Heidelberg, Mannheim, Germany
[61] Faculty of Applied Information Science, Hiroshima Institute of Technology, Hiroshima, Japan
[62] [(a)] Department of Physics, The Chinese University of Hong Kong, Shatin, N.T., Hong Kong; [(b)] Department of Physics, The University of Hong Kong, Hong Kong; [(c)] Department of Physics and Institute for Advanced Study, The Hong Kong University of Science and Technology, Clear Water Bay, Kowloon, Hong Kong, China
[63] Department of Physics, Indiana University, Bloomington IN, United States of America
[64] Institut für Astro- und Teilchenphysik, Leopold-Franzens-Universität, Innsbruck, Austria
[65] University of Iowa, Iowa City IA, United States of America
[66] Department of Physics and Astronomy, Iowa State University, Ames IA, United States of America
[67] Joint Institute for Nuclear Research, JINR Dubna, Dubna, Russia
[68] KEK, High Energy Accelerator Research Organization, Tsukuba, Japan
[69] Graduate School of Science, Kobe University, Kobe, Japan
[70] Faculty of Science, Kyoto University, Kyoto, Japan
[71] Kyoto University of Education, Kyoto, Japan
[72] Department of Physics, Kyushu University, Fukuoka, Japan
[73] Instituto de Física La Plata, Universidad Nacional de La Plata and CONICET, La Plata, Argentina
[74] Physics Department, Lancaster University, Lancaster, United Kingdom
[75] [(a)] INFN Sezione di Lecce; [(b)] Dipartimento di Matematica e Fisica, Università del Salento, Lecce, Italy
[76] Oliver Lodge Laboratory, University of Liverpool, Liverpool, United Kingdom
[77] Department of Physics, Jožef Stefan Institute and University of Ljubljana, Ljubljana, Slovenia
[78] School of Physics and Astronomy, Queen Mary University of London, London, United Kingdom
[79] Department of Physics, Royal Holloway University of London, Surrey, United Kingdom
[80] Department of Physics and Astronomy, University College London, London, United Kingdom
[81] Louisiana Tech University, Ruston LA, United States of America
[82] Laboratoire de Physique Nucléaire et de Hautes Energies, UPMC and Université Paris-Diderot and CNRS/IN2P3, Paris, France
[83] Fysiska institutionen, Lunds universitet, Lund, Sweden
[84] Departamento de Fisica Teorica C-15, Universidad Autonoma de Madrid, Madrid, Spain
[85] Institut für Physik, Universität Mainz, Mainz, Germany
[86] School of Physics and Astronomy, University of Manchester, Manchester, United Kingdom
[87] CPPM, Aix-Marseille Université and CNRS/IN2P3, Marseille, France
[88] Department of Physics, University of Massachusetts, Amherst MA, United States of America
[89] Department of Physics, McGill University, Montreal QC, Canada
[90] School of Physics, University of Melbourne, Victoria, Australia
[91] Department of Physics, The University of Michigan, Ann Arbor MI, United States of America
[92] Department of Physics and Astronomy, Michigan State University, East Lansing MI, United States of America
[93] [(a)] INFN Sezione di Milano; [(b)] Dipartimento di Fisica, Università di Milano, Milano, Italy
[94] B.I. Stepanov Institute of Physics, National Academy of Sciences of Belarus, Minsk, Republic of Belarus
[95] National Scientific and Educational Centre for Particle and High Energy Physics, Minsk, Republic of Belarus
[96] Group of Particle Physics, University of Montreal, Montreal QC, Canada
[97] P.N. Lebedev Physical Institute of the Russian Academy of Sciences, Moscow, Russia
[98] Institute for Theoretical and Experimental Physics (ITEP), Moscow, Russia
[99] National Research Nuclear University MEPhI, Moscow, Russia
[100] D.V. Skobeltsyn Institute of Nuclear Physics, M.V. Lomonosov Moscow State University, Moscow, Russia
[101] Fakultät für Physik, Ludwig-Maximilians-Universität München, München, Germany
[102] Max-Planck-Institut für Physik (Werner-Heisenberg-Institut), München, Germany
[103] Nagasaki Institute of Applied Science, Nagasaki, Japan
[104] Graduate School of Science and Kobayashi-Maskawa Institute, Nagoya University, Nagoya, Japan
[105] [(a)] INFN Sezione di Napoli; [(b)] Dipartimento di Fisica, Università di Napoli, Napoli, Italy
[106] Department of Physics and Astronomy, University of New Mexico, Albuquerque NM, United States of America

[107] *Institute for Mathematics, Astrophysics and Particle Physics, Radboud University Nijmegen/Nikhef, Nijmegen, Netherlands*
[108] *Nikhef National Institute for Subatomic Physics and University of Amsterdam, Amsterdam, Netherlands*
[109] *Department of Physics, Northern Illinois University, DeKalb IL, United States of America*
[110] *Budker Institute of Nuclear Physics, SB RAS, Novosibirsk, Russia*
[111] *Department of Physics, New York University, New York NY, United States of America*
[112] *Ohio State University, Columbus OH, United States of America*
[113] *Faculty of Science, Okayama University, Okayama, Japan*
[114] *Homer L. Dodge Department of Physics and Astronomy, University of Oklahoma, Norman OK, United States of America*
[115] *Department of Physics, Oklahoma State University, Stillwater OK, United States of America*
[116] *Palacký University, RCPTM, Olomouc, Czech Republic*
[117] *Center for High Energy Physics, University of Oregon, Eugene OR, United States of America*
[118] *LAL, Univ. Paris-Sud, CNRS/IN2P3, Université Paris-Saclay, Orsay, France*
[119] *Graduate School of Science, Osaka University, Osaka, Japan*
[120] *Department of Physics, University of Oslo, Oslo, Norway*
[121] *Department of Physics, Oxford University, Oxford, United Kingdom*
[122] *[(a)] INFN Sezione di Pavia; [(b)] Dipartimento di Fisica, Università di Pavia, Pavia, Italy*
[123] *Department of Physics, University of Pennsylvania, Philadelphia PA, United States of America*
[124] *National Research Centre "Kurchatov Institute" B.P.Konstantinov Petersburg Nuclear Physics Institute, St. Petersburg, Russia*
[125] *[(a)] INFN Sezione di Pisa; [(b)] Dipartimento di Fisica E. Fermi, Università di Pisa, Pisa, Italy*
[126] *Department of Physics and Astronomy, University of Pittsburgh, Pittsburgh PA, United States of America*
[127] *[(a)] Laboratório de Instrumentação e Física Experimental de Partículas - LIP, Lisboa; [(b)] Faculdade de Ciências, Universidade de Lisboa, Lisboa; [(c)] Department of Physics, University of Coimbra, Coimbra; [(d)] Centro de Física Nuclear da Universidade de Lisboa, Lisboa; [(e)] Departamento de Fisica, Universidade do Minho, Braga; [(f)] Departamento de Fisica Teorica y del Cosmos and CAFPE, Universidad de Granada, Granada (Spain); [(g)] Dep Fisica and CEFITEC of Faculdade de Ciencias e Tecnologia, Universidade Nova de Lisboa, Caparica, Portugal*
[128] *Institute of Physics, Academy of Sciences of the Czech Republic, Praha, Czech Republic*
[129] *Czech Technical University in Prague, Praha, Czech Republic*
[130] *Faculty of Mathematics and Physics, Charles University in Prague, Praha, Czech Republic*
[131] *State Research Center Institute for High Energy Physics (Protvino), NRC KI, Russia*
[132] *Particle Physics Department, Rutherford Appleton Laboratory, Didcot, United Kingdom*
[133] *[(a)] INFN Sezione di Roma; [(b)] Dipartimento di Fisica, Sapienza Università di Roma, Roma, Italy*
[134] *[(a)] INFN Sezione di Roma Tor Vergata; [(b)] Dipartimento di Fisica, Università di Roma Tor Vergata, Roma, Italy*
[135] *[(a)] INFN Sezione di Roma Tre; [(b)] Dipartimento di Matematica e Fisica, Università Roma Tre, Roma, Italy*
[136] *[(a)] Faculté des Sciences Ain Chock, Réseau Universitaire de Physique des Hautes Energies - Université Hassan II, Casablanca; [(b)] Centre National de l'Energie des Sciences Techniques Nucleaires, Rabat; [(c)] Faculté des Sciences Semlalia, Université Cadi Ayyad, LPHEA-Marrakech; [(d)] Faculté des Sciences, Université Mohamed Premier and LPTPM, Oujda; [(e)] Faculté des sciences, Université Mohammed V, Rabat, Morocco*
[137] *DSM/IRFU (Institut de Recherches sur les Lois Fondamentales de l'Univers), CEA Saclay (Commissariat à l'Energie Atomique et aux Energies Alternatives), Gif-sur-Yvette, France*
[138] *Santa Cruz Institute for Particle Physics, University of California Santa Cruz, Santa Cruz CA, United States of America*
[139] *Department of Physics, University of Washington, Seattle WA, United States of America*
[140] *School of Physics, Shandong University, Shandong, China*
[141] *Department of Physics and Astronomy, Shanghai Key Laboratory for Particle Physics and Cosmology, Shanghai Jiao Tong University, Shanghai; (also affiliated with PKU-CHEP), China*
[142] *Department of Physics and Astronomy, University of Sheffield, Sheffield, United Kingdom*
[143] *Department of Physics, Shinshu University, Nagano, Japan*
[144] *Fachbereich Physik, Universität Siegen, Siegen, Germany*

JHEP04(2017)086

[145] Department of Physics, Simon Fraser University, Burnaby BC, Canada
[146] SLAC National Accelerator Laboratory, Stanford CA, United States of America
[147] [(a)] Faculty of Mathematics, Physics & Informatics, Comenius University, Bratislava; [(b)] Department of Subnuclear Physics, Institute of Experimental Physics of the Slovak Academy of Sciences, Kosice, Slovak Republic
[148] [(a)] Department of Physics, University of Cape Town, Cape Town; [(b)] Department of Physics, University of Johannesburg, Johannesburg; [(c)] School of Physics, University of the Witwatersrand, Johannesburg, South Africa
[149] [(a)] Department of Physics, Stockholm University; [(b)] The Oskar Klein Centre, Stockholm, Sweden
[150] Physics Department, Royal Institute of Technology, Stockholm, Sweden
[151] Departments of Physics & Astronomy and Chemistry, Stony Brook University, Stony Brook NY, United States of America
[152] Department of Physics and Astronomy, University of Sussex, Brighton, United Kingdom
[153] School of Physics, University of Sydney, Sydney, Australia
[154] Institute of Physics, Academia Sinica, Taipei, Taiwan
[155] Department of Physics, Technion: Israel Institute of Technology, Haifa, Israel
[156] Raymond and Beverly Sackler School of Physics and Astronomy, Tel Aviv University, Tel Aviv, Israel
[157] Department of Physics, Aristotle University of Thessaloniki, Thessaloniki, Greece
[158] International Center for Elementary Particle Physics and Department of Physics, The University of Tokyo, Tokyo, Japan
[159] Graduate School of Science and Technology, Tokyo Metropolitan University, Tokyo, Japan
[160] Department of Physics, Tokyo Institute of Technology, Tokyo, Japan
[161] Tomsk State University, Tomsk, Russia
[162] Department of Physics, University of Toronto, Toronto ON, Canada
[163] [(a)] INFN-TIFPA; [(b)] University of Trento, Trento, Italy
[164] [(a)] TRIUMF, Vancouver BC; [(b)] Department of Physics and Astronomy, York University, Toronto ON, Canada
[165] Faculty of Pure and Applied Sciences, and Center for Integrated Research in Fundamental Science and Engineering, University of Tsukuba, Tsukuba, Japan
[166] Department of Physics and Astronomy, Tufts University, Medford MA, United States of America
[167] Department of Physics and Astronomy, University of California Irvine, Irvine CA, United States of America
[168] [(a)] INFN Gruppo Collegato di Udine, Sezione di Trieste, Udine; [(b)] ICTP, Trieste; [(c)] Dipartimento di Chimica, Fisica e Ambiente, Università di Udine, Udine, Italy
[169] Department of Physics and Astronomy, University of Uppsala, Uppsala, Sweden
[170] Department of Physics, University of Illinois, Urbana IL, United States of America
[171] Instituto de Fisica Corpuscular (IFIC) and Departamento de Fisica Atomica, Molecular y Nuclear and Departamento de Ingeniería Electrónica and Instituto de Microelectrónica de Barcelona (IMB-CNM), University of Valencia and CSIC, Valencia, Spain
[172] Department of Physics, University of British Columbia, Vancouver BC, Canada
[173] Department of Physics and Astronomy, University of Victoria, Victoria BC, Canada
[174] Department of Physics, University of Warwick, Coventry, United Kingdom
[175] Waseda University, Tokyo, Japan
[176] Department of Particle Physics, The Weizmann Institute of Science, Rehovot, Israel
[177] Department of Physics, University of Wisconsin, Madison WI, United States of America
[178] Fakultät für Physik und Astronomie, Julius-Maximilians-Universität, Würzburg, Germany
[179] Fakultät für Mathematik und Naturwissenschaften, Fachgruppe Physik, Bergische Universität Wuppertal, Wuppertal, Germany
[180] Department of Physics, Yale University, New Haven CT, United States of America
[181] Yerevan Physics Institute, Yerevan, Armenia
[182] Centre de Calcul de l'Institut National de Physique Nucléaire et de Physique des Particules (IN2P3), Villeurbanne, France

JHEP04(2017)086

[a] Also at Department of Physics, King's College London, London, United Kingdom
[b] Also at Institute of Physics, Azerbaijan Academy of Sciences, Baku, Azerbaijan
[c] Also at Novosibirsk State University, Novosibirsk, Russia
[d] Also at TRIUMF, Vancouver BC, Canada
[e] Also at Department of Physics & Astronomy, University of Louisville, Louisville, KY, United States of America
[f] Also at Physics Department, An-Najah National University, Nablus, Palestine
[g] Also at Department of Physics, California State University, Fresno CA, United States of America
[h] Also at Department of Physics, University of Fribourg, Fribourg, Switzerland
[i] Also at Departament de Fisica de la Universitat Autonoma de Barcelona, Barcelona, Spain
[j] Also at Departamento de Fisica e Astronomia, Faculdade de Ciencias, Universidade do Porto, Portugal
[k] Also at Tomsk State University, Tomsk, Russia, Russia
[l] Also at Universita di Napoli Parthenope, Napoli, Italy
[m] Also at Institute of Particle Physics (IPP), Canada
[n] Also at National Institute of Physics and Nuclear Engineering, Bucharest, Romania
[o] Also at Department of Physics, St. Petersburg State Polytechnical University, St. Petersburg, Russia
[p] Also at Department of Physics, The University of Michigan, Ann Arbor MI, United States of America
[q] Also at Centre for High Performance Computing, CSIR Campus, Rosebank, Cape Town, South Africa
[r] Also at Louisiana Tech University, Ruston LA, United States of America
[s] Also at Institucio Catalana de Recerca i Estudis Avancats, ICREA, Barcelona, Spain
[t] Also at Graduate School of Science, Osaka University, Osaka, Japan
[u] Also at Department of Physics, National Tsing Hua University, Taiwan
[v] Also at Institute for Mathematics, Astrophysics and Particle Physics, Radboud University Nijmegen/Nikhef, Nijmegen, Netherlands
[w] Also at Department of Physics, The University of Texas at Austin, Austin TX, United States of America
[x] Also at CERN, Geneva, Switzerland
[y] Also at Georgian Technical University (GTU),Tbilisi, Georgia
[z] Also at Ochadai Academic Production, Ochanomizu University, Tokyo, Japan
[aa] Also at Manhattan College, New York NY, United States of America
[ab] Also at Academia Sinica Grid Computing, Institute of Physics, Academia Sinica, Taipei, Taiwan
[ac] Also at School of Physics, Shandong University, Shandong, China
[ad] Also at Department of Physics, California State University, Sacramento CA, United States of America
[ae] Also at Moscow Institute of Physics and Technology State University, Dolgoprudny, Russia
[af] Also at section de Physique, Université de Genève, Geneva, Switzerland
[ag] Also at Eotvos Lorand University, Budapest, Hungary
[ah] Also at Departments of Physics & Astronomy and Chemistry, Stony Brook University, Stony Brook NY, United States of America
[ai] Also at International School for Advanced Studies (SISSA), Trieste, Italy
[aj] Also at Department of Physics and Astronomy, University of South Carolina, Columbia SC, United States of America
[ak] Also at Institut de Física d'Altes Energies (IFAE), The Barcelona Institute of Science and Technology, Barcelona, Spain
[al] Also at School of Physics and Engineering, Sun Yat-sen University, Guangzhou, China
[am] Also at Institute for Nuclear Research and Nuclear Energy (INRNE) of the Bulgarian Academy of Sciences, Sofia, Bulgaria
[an] Also at Faculty of Physics, M.V.Lomonosov Moscow State University, Moscow, Russia
[ao] Also at Institute of Physics, Academia Sinica, Taipei, Taiwan
[ap] Also at National Research Nuclear University MEPhI, Moscow, Russia
[aq] Also at Department of Physics, Stanford University, Stanford CA, United States of America
[ar] Also at Institute for Particle and Nuclear Physics, Wigner Research Centre for Physics, Budapest, Hungary
[as] Also at Flensburg University of Applied Sciences, Flensburg, Germany
[at] Also at University of Malaya, Department of Physics, Kuala Lumpur, Malaysia
[au] Also at CPPM, Aix-Marseille Université and CNRS/IN2P3, Marseille, France
[*] Deceased